

國立交通大學

電子工程學系電子研究所

博士論文

高性能離子感應電晶體之可靠度研究及應用



Reliability Investigation and Application of High
Performance Ion-Sensitive Field Effect Transistors

研究生：趙高毅

Kuo-Yi Chao

指導教授：張國明博士

Dr. Kow-Ming Chang

高性能離子感應電晶體之可靠度研究及應用

Reliability Investigation and Application of High
Performance Ion-Sensitive Field Effect Transistors

研究生：趙高毅

Student : Kuo-Yi Chao

指導教授：張國明博士

Advisor : Dr. Kow-Ming Chang



A Dissertation
Submitted to Institute of Electronics
College of Electrical Engineering and Computer Science
National Chiao Tung University
in partial Fulfillment of Requirements
for the Degree of
Doctor of Philosophy
in
Electronics Engineering

September 2007
Hsinchu, Taiwan, Republic of China

中華民國九十六年九月

高性能離子感應電晶體之可靠度研究及應用

研究生:趙高毅

指導教授:張國明 博士

國立交通大學

電子工程學系暨電子研究所

博士論文

摘要

本論文提出使用二氧化鋯 (ZrO_2) 作為離子感應場效電晶體 (ISFET) 之感應層，並嘗試去調控溫度與製程參數對 ISFET 的影響，當我們可以得到一個穩定的感測靈敏度則因為漂移效應所造成的水合深度就可獲得，當我們瞭解漂移效應後，我們提出兩種方法來解決此種負面效應。

在第二章中先描述離子感應場效電晶體 (ISFET) 的理論跟模型，例如，表面鍵結分離模型、Gouy-Chapman 理論、Gouy-Chapman-Stern 理論、與漂移理論。

在第三章的研究裡，氧化鋯成功的應用在離子感應場效電晶體 (ISFET) 裡，成為酸鹼感測層，再利用 HP4156A 以定電流量測方式後，可得到相當高的反應範圍，其感測靈敏度介於 $56.7 \sim 58.3$ mV/pH 之間。這裡所使用的氧化鋯薄膜是使用直流濺鍍方式所沈積的，此薄膜對氧化層跟矽晶都具有相當好的吸附特性，當感測環境加入 1 莫耳體積濃度的氯化鈉容液以後，感應靈敏度會有些微的減少，不過還是具有相當好的線性度及 52.5 mV/pH 的靈敏度。

在論文的第四章中，我們利用參考場效電晶體 (REFET) 來控制溫度跟製程差異的影響，當我們利用參考場效電晶體 (REFET) 校正輸出訊號後，就可以得

到一個相當穩定的感應靈敏度並可以得到以二氧化矽為感測層的離子感應場效電晶體 (ISFET) 的初始本質漂移 (intrinsic drift), 更進而定義出因為漂移影響所造成的水合層厚度。從實驗的結果來看, 用二氧化矽感測層所做成的離子感應場效電晶體 (ISFET) 水合深度大約為 50 奈米, 而實驗當中所測出來的感測反應也很穩定, 大約處於 28~32 mV/pH 之間, 使用這方法可以很簡單的找出水合深度, 這將對探討漂移效應的真正機制有所助益。

當我們瞭解漂移現象以後, 我們就試著設計兩種方法來減少這個效應, 其中一種方法是在第五章, 在這章節當中, 我們提出漂移跟閘極電壓的關係, 從而設計出一種簡單且便宜的方法來解決漂移問題。我們利用參考電極來施加不同的定電壓在感測層上面, 就可以很明顯的看出閘極的飄移電壓跟應力電壓的強烈相關性, 當閘極電壓控制在 0.5 伏特, 就可以使得以二氧化矽為感測層的離子感應場效電晶體之飄移電壓從原來的十小時飄移 56.12 mV 變為 2.94 mV, 其改善百分率高達 94.8%。又當閘極電壓被控制在-1 伏特的時候, 就可以使得以二氧化鋯為感測層的離子感應場效電晶體 (ISFET) 之飄移電壓從原來的十小時飄移-57.94 mV 變為 0.76 mV, 其改善百分率高達 98.7%。

另一個解決方法提出於本論文的第六章中, 其方法為利用參考感應場效電晶體 (REFET) 來減少飄移效應, 首先是利用鉍電漿去處理一個以二氧化鋯為感應薄膜的離子感應場效電晶體 (ISFET), 以得到一個簡單且跟互補金屬氧化電晶體相容的參考感測場效電晶體 (REFET) 來量測酸鹼性。這是一個獨創且具有很高的可塑性, 可以整合離子感應場效電晶體 (ISFET) 到化學微系統, 應用於生物體分析或整合到單晶片系統當中。當我們利用 4156A 以定電流量測方式時, 可以同時得到離子感應場效電晶體 (ISFET)、參考感應場效電晶體 (REFET) 及兩者間的差值感應靈敏度。這個以二氧化鋯為感測層的離子感應場效電晶體 (ISFET) 具有很高的離子感測能力, 其範圍介於 56.7~58.3 mV/pH 間, 其變異度為 3%, 又參考感應場效電晶體 (REFET) 具有較小的離子感測能力, 其範圍介於 27.6~29 mV/pH 間, 其變異度為 5%。當我們使用離子感應場效電晶體/參

考感應場效電晶體(ISFET/REFET)差值電壓對的時候，可以得到一個非常穩定的差值感應靈敏度，其範圍介於 29.1~29.3 mV/pH 間，其變異度為 0.7%。這個結果告訴我們，這個研究不僅使得離子感應場效電晶體（ISFET）可以整合到微系統當中，也可以增加感應靈敏度的穩定性。



Reliability Investigation and Application of High Performance Ion-Sensitive Field Effect Transistors

Student: Kuo-Yi Chao

Advisor: Dr. Kow-Ming Chang

Department of electronics Engineering & Institute of Electronics
National Chiao Tung University



Abstract

This dissertation proposes to use zirconium oxide as a membrane of ion-sensitive field effective transistor (ISFET), and to control the effects of temperature and process deviation. When a stable sensitivity and intrinsic drift of SiO₂ gate ISFET can be found, the thickness of hydration layer that is introduced by the drift effect will be found, too. After we understand the drift effect, we also propose two methods to solve the unwanted effect.

In Chapter 2, theories and models of ISFET are described, including site-dissociation model, Gouy-Chapman theory, Gouy-Chapman-Stern theory, and drift model.

Chapter 3 describes the application of the zirconium oxide (ZrO₂) membrane as a pH-sensitive layer for ISFETs. It exhibited an excellent response range of 56.7~58.3 mV/pH from the fixed current measurement using HP4156A. The ZrO₂ membrane

prepared by direct current (DC) sputtering was used as a pH-sensitive film that showed good surface adsorption with oxide and silicon. The pH sensitivities slightly decreased in 1 M NaCl solution; however, the device showed a perfect linear response of 52.5 mV/pH.

In Chapter 4, a reference field effective transistor (REFET) is used to control the effects of temperature and process deviation. After the calibration of REFET, a very stable sensitivity and intrinsic drift of SiO₂ gate ISFET can be obtained. It can be used to define the thickness of hydration layer that is introduced by the drift effect. Results of this study will show that the thickness of hydration is about 50 nm in SiO₂ membrane ISFET. It exhibits a stable response of 28~32 mV/pH from the fixed current measurement by HP4156A. This method is a really simple way to find the thickness of hydration layer, and it will be useful in the study of the real mechanism in drift effect.

When we understand the phenomenon of drift, we try to design two methods to reduce this effect. One is in Chapter 5. A simple and cheap way to solve the drift problem is presented which describes the relation of drift and gate voltage. Constant various gate voltages are biased in sensing layers with reference electrode. It obviously shows a strong relation of gate drifts and gate stress voltages. When the gate voltage is controlled as 0.5 V, the drift voltage of SiO₂ gate ISFET will decrease from 56.12 to 2.94 mV in ten hours measurement. The improvement of drift voltage reaches 94.8%. When the gate voltage is controlled as -1 V, the drift voltage of ZrO₂ gate ISFET will also decrease from -57.94 to 0.76 mV. The improvement of drift voltage reaches 98.7%.

Another one in Chapter 6 of the thesis is using REFET to reduce the drift effect. A simple CMOS compatible REFET for pH detection by post NH₃ plasma surface treatment of a ZrO₂ membrane ISFET has been developed. It is a novel study that has

latent capacity to integrate the ISFET devices into a chemical micro system for in vivo analysis or become a part of lab-on-a-chip. With the fixed current measurement by HP4156, we can get not only the individual sensitivities of ISFET and REFET, but also the differential sensitivities of ISFET/REFET pair. The ZrO₂ membrane ISFET exhibits an excellent response of 56.7~58.3mV/pH with deviation of 3% and the REFET shows a small response of 27.6~29 mV/pH with a deviation of 5%. Using this ISFET/REFET differential pair, we can get a very stable differential sensitivities of 29.1~29.3 mV/pH with a small deviation of 0.7%. This result indicates that the research not only makes the ISFET integrate into a micro system in a simple way possible, but also increases the stability of sensitivity.



Acknowledgement

一轉眼，幾年的時間就過了，期間交錯著無數的酸甜苦辣，不過一路走來總算是水到渠成，也算是不負所望，對於多年來，從碩士到博士一路悉心照料的指導教授張國明博士，心中充滿無數的感激。由於老師自由的寬宏指導方式，因而增加了學生的思考力與創造力，也由於老師的淵博學識，因而提供了學生無數的建議與幫助，更難能可貴是，老師總是諄諄教誨學生待人處事的態度，也培養學生積極樂觀的態度，讓學生受益良多。另外，桂正楣教授在這段時間內亦提供學生大量的協助與關心，在此，學生由衷的感謝兩位教授多年來的包容照顧。

在研究的日子裡，總需要各式各樣的協助與幫忙，特別感謝實驗室的學長楊知一、鄧一中、鄭兆禎、鍾元鴻、楊文誌、王敬業、游凱翔、陳在洸，同學朱俊宜、林俊銘，學弟郭俊銘、林昆鋒、張知天、吳鼎文、傅傳旭、吳冠增、黃俊皓、許信佑、周庭韋、黃明欽、林佳鴻、陳敬昱、鄧至剛、室友王律堯及不勝枚舉的實驗室成員，因為有你們的貢獻與協助，使得此研究可以順利進行，也因為你們的存在，為我的研究生涯添加大量的色彩。另外，對於 NDL、奈米中心、及系辦的職員亦多所感謝，謝謝你們多年來的熱心服務。

最後當然要感謝最重要的人，就是生我、養我、育我、教我的父母及兄姐，沒有你們過去的培育、付出，就不會有今天的我，對於女友一路的陪伴及鼓勵亦是我往前走的原動力，僅以此文致謝所有我身邊的人。

Contents

Abstract (Chinese)	i
Abstract (English)	iv
Acknowledgement	vii
Contents	viii
Table Captions	xii
Figure Captions	xiii

Chapter 1 Introduction

1.1 ISFETs.....	1
1.2 ChemFETs and ENFETS.....	2
1.3 REFETs.....	3
1.4 Applications.....	4
1.5 Outline of the Thesis.....	4
1.6 References.....	7



Chapter 2 Theory and Principle

2.1 ISFET's Model.....	14
2.2 The Site-Dissociation Model.....	16
2.3 The Gouy-Chapman Theory.....	19
2.4 The Gouy-Chapman-Stern Theory.....	20
2.5 Site-Dissociation and Gouy-Chapman-Stern Model.....	20
2.6 Physical Model for Drift.....	21
2.7 References.....	25

Chapter 3 Characteristics of Zirconium Oxide (ZrO₂) Gate Ion-Sensitive

Field-Effect Transistors

3.1 Backgrounds and Motivation.....	32
3.2 Experimental Procedure.....	33
3.2.1 Device Fabrication.....	33
3.2.2 Packaging and Measurement.....	34
3.3 Results and Discussion.....	34
3.3.1 I _D -V _{DS} Characteristics of ZrO ₂ Gate ISFETs.....	34
3.3.2 pH Sensitivity of ZrO ₂ Gate ISFET.....	35
3.3.3 Ratio of Width to Length in Channel Affecting ZrO ₂ Gate ISFET.....	35
3.3.4 Drift of ZrO ₂ Gate ISFET.....	35
3.3.5 pH Sensitivity of ZrO ₂ Membrane ISFET in 1 M NaCl Solution.....	36
3.4 Conclusions.....	36
3.5 References	37

Chapter 4 Drift Characteristics with Sensing Oxide Thickness Modulation by Co-fabricating ISFET and REFET

4.1 Backgrounds and Motivation.....	49
4.2 Experimental Procedure.....	50
4.2.1 Device Fabrication.....	50
4.2.2 Packaging and Measurement.....	51
4.3 Results and Discussion.....	51
4.3.1 pH Sensitivity of the ISFET/REFET.....	51

4.3.2 Drift of the SiO ₂ Gate ISFET.....	52
4.4 Conclusion.....	52
4.5 References.....	54

Chapter 5 Ultra-Low Drift Voltage by Using Gate Voltage Control in Oxide-Based Gate ISFET

5.1 Backgrounds and Motivation.....	62
5.2 Experimental Procedure.....	63
5.2.1 Device Fabrication.....	64
5.2.2 Packaging and Measurement.....	64
5.3 Results and Discussion.....	65
5.3.1 I _D -V _{DS} Characteristics of the ISFET Devices.....	65
5.3.2 pH Sensitivities of the ISFETs.....	65
5.3.3 Drift of ISFET.....	66
5.4 Conclusion.....	67
5.5 References.....	68



Chapter 6 A Simple CMOS Compatible REFET for pH Detection by Post NH₃

Plasma Surface Treatment of ISFET

6.1 Backgrounds and Motivation.....	77
6.2 Experimental Procedure.....	78
6.2.1 Device Fabrication.....	78
6.2.2 Packaging and Measurement.....	78
6.3 Results and Discussion.....	79
6.3.1 The pH Sensitivity of the ZrO ₂ Gate ISFET.....	80

6.3.2 The pH Sensitivity of the ZrO ₂ Gate REFET.....	80
6.4 Conclusion.....	81
6.5 References.....	82
Chapter 7 Conclusions and Future Prospects	
7.1 Conclusions.....	88
7.2 Future Prospects.....	89



Table Captions

Chapter 2

Table 2-I Sensitivities and test range for the different sensing membranes.....27

Chapter 3

Table 3-I Growth conditions for film deposition using sputtering system.....39



Figure Captions

Chapter 2

Figure 2-1 The similarities and differences between MOSFET and ISFET devices. It can be seen that the reference electrode, the aqueous solution and the phenomena occurring at the oxide-solution interface must be accounted for instead of Φ_M/q28

Figure 2-2 Potential profile and charge distribution at an oxide electrolyte solution interface (After Siu et al., Ref. 2).....29

Figure 2-3 Schematic representation of site-dissociation model.....30

Figure 2-4 Series combination of the (a) initial (b) hydrated insulator capacitance...31

Chapter 3

Figure 3-1 Schematic diagram of ZrO_2 gate ISFET fabricated by MOSFET technique.....40

Figure 3-2 Setup of measurement using HP4156A semiconductor parameter analyzer and temperature controller.....41

Figure 3-3 $I_{DS}-V_{DS}$ curves of ZrO_2 gate ISFETs.....42

Figure 3-4 $I_{DS}-V_{GS}$ curves that are shifted parallel with pH concentration of buffer solutions, and in nonsaturation region with $V_{DS} = 2 V$43

Figure 3-5 V_{GS} and pH values for obtaining pH response of 57.5 mV/pH from slope of linear-fitted line.....44

Figure 3-6 Sensitivities of three devices having different ratios of width to length...45

Figure 3-7 Drift of 5.82 mV during 7 h measurement in which a drift of 0.831 mV/h is obtained.....46

Figure 3-8 Long-term drift of about 85 mV during 200 h measurement in which a drift

of 0.425 mV/h is obtained.....	47
Figure 3-9 V_{GS} and pH values in 1M NaCl solution for obtaining pH response of 52.5 mV/pH from slope of linear-fitted line.....	48

Chapter 4

Figure 4-1 The schematic diagram of the SiO ₂ gate ISFET which is fabricated by the MOSFET technique.....	56
Figure 4-2 The set up of measurement with the HP4156A semiconductor parameter analyzer and temperature controller.....	57
Figure 4-3 (a) The I_{DS} - V_{GS} curves of SiO ₂ gate ISFET devices (50 nm).....	58
(b) The I_{DS} - V_{GS} curves of Ta ₂ O ₅ gate ISFET devices (30 nm).....	58
Figure 4-4 The V_{GS} to pH values that can obtain the pH response by the slope of the linear fitted line. (a)33.15 mV/pH of SiO ₂ gate ISFET devices (50 nm). (b) 55.66 mV/pH of Ta ₂ O ₅ gate ISFET devices (30 nm).....	59
Figure 4-5 Drifts in ISFET and REFET during 7 hours.....	60
Figure 4-6 Delta drifts of SiO ₂ gate ISFET devices.....	61

Chapter 5

Figure 5-1 Series combinations of (a) initial, (b) hydrated without gate voltage control, and (c) hydrated with gate voltage control.....	69
Figure 5-2 Fabricated processes of ISFET which is a CMOS compatible technique..	70
Figure 5-3 Setup of measurement Using HP4156A semiconductor parameter analyzer and temperature controller.....	71
Figure 5-4 (a) I_D - V_{DS} curves of SiO ₂ gate ISFETs.....	72
Figure 5-4 (b) I_D - V_{DS} curves of ZrO ₂ gate ISFETs.....	72
Figure 5-5 (a) I_D - V_{GS} curves of SiO ₂ gate ISFETs.....	73

Figure 5-5 (b) I_D - V_{GS} curves of ZrO_2 gate ISFETs.....	73
Figure 5-6 (a) Sensitivity of SiO_2 gate ISFETs.....	74
Figure 5-6 (b) Sensitivity of ZrO_2 gate ISFETs.....	74
Figure 5-7 (a) Drift of SiO_2 gate ISFET with time.....	75
Figure 5-8 (b) Drift of ZrO_2 gate ISFET with time.....	75
Figure 5-9 Relation of drift voltages and gate stress voltages.....	76

Chapter 6

Figure 6-1 The schematic diagram of the ZrO_2 gate ISFET that is fabricated by the MOSFET technique.....	84
Figure 6-2 The set up of measurement with the HP 4156A Semiconductor Parameter Analyzer and Temperature controller.....	85
Figure 6-3 (a) The I_{DS} - V_{GS} curves that are shifted in parallel with the pH concentration of the buffer solutions, and in the non-saturation region with $V_{DS} = 2V$	86
Figure 6-3 (b) The V_{GS} to pH values that can obtain a median pH response of 57.5 mV/pH by the slope of the linear fitted line.....	86
Figure 6-4 The sensitivities to post NH_3 plasma treatment time output characteristics of the ISFET(W/O Plasma), REFET(W/ Plasma) and ISFET/REFET pair (Differential Sensitivities) devices with $V_{DS}= 2V$ and drain current at 527 μA	87

Chapter 1

Introduction

1.1 ISFETs

In the literature relating to ion-selective field-effect Transistors (ISFETs), the 1970's paper of Bergveld is cited as the first paper [1]. The ISFET is introduced as a new device that combines the chemical-sensitive properties of glass membranes with the characteristics of the metal-oxide-semiconductor field-effect transistors (MOSFET) device. ISFET is a special type of MOSFET without a metal gate, in which the gate is directly exposed to the buffer solution. When there is a change in the surface potential between the gate insulator and the electrolyte, the electric field at the insulator semiconductor interface will be changed and the channel conductance that affects the drain current will also be modulated. Since the channel conductance and drain current can be modulated, we may measure the changes by applying a fixed source to drain voltage or a constant source to drain voltage current and different output gate voltages. By these methods, we can plot a standard linear line between gate voltages and various pH values, and a standard linear line can be taken to measure an unknown acid or an alkaline solution. Compared with the conventional method, ISFET has some advantages such as small size, short-response time, low cost, and complementary metal-oxide-semiconductor (CMOS) compatible processes.

The development of ISFET has been on going for more than 35 years, and the first sensitive membrane used is silicon dioxide (SiO_2), which showed an unstable sensitivity and a large drift. Subsequently, Al_2O_3 , Ta_2O_5 , SnO_2 , TiN , $\alpha\text{-WO}_3$, indium tin oxide (ITO), and ZrO_2 were used as pH-sensitive membranes to achieve a higher pH response and a more stable drift voltage [2~9]. Also some explanations of the mechanisms of operation of the ISFETs [10-16] are appearing. The physical-chemical

models to be used with semiconductor-based devices simulation problems are developed [17-22]. Initially developed for pH detection, ISFETs were also proposed for biomedical, agriculture, environmental, general analytical applications, and food industry [23-34]. However, further improvements and investigations of ISFET performances are needed to promote their use in microsystems for specific applications. Difficulties arise not only from technological issues, but also from the lack of considering first-order mechanisms such as the effects of drift, hysteresis, and temperature. These limiting operating conditions are particularly relevant in respect of possible applications of ISFET-based microsystems in industrial control and monitoring of processes (e.g. biofermenters for biotechnological applications) or where temperature cannot be a controlled parameter.

In this study, a simple and cheap way to solve the drift problem is presented which describes the relation of drift and gate voltage. Constant various gate voltages are biased in the sensing layer with reference electrode. It obviously shows a strong relation of gate drift and gate stress voltages. A great improvement of drift voltage can be achieved by using gate voltage controlling method.

1.2 ChemFETs and ENFETs

The classes of chemical sensors that use the FET as an underlying amplification method are called ChemFETs. A variety of ChemFET structures have been proposed and demonstrated. However, the most common class of ChemFETs in both commercial and research uses is the ISFET. The ISFET is characterized by the absence of an explicit gate material; the insulating layer in the FET structure is used as the chemically sensitive layer instead. When the insulator layer is sensitive to enzymes and the gate layer is missing from the FET structure, the resulting ChemFET structure is typically called an enzyme selective FET (ENFET). All ChemFET based

structures work on the basic principle of measuring surface charge changes at the interface between the insulator layer and the overlying layer. Changes in surface charges result in changes in the work function that are in turn, measured as a change in transistor threshold voltage.

1.3 REFETs

A conventional reference electrode (e. g. Ag/AgCl electrode) is always used in the measurement system. If we want to integrate the ISFET devices into a chemical micro system for in vivo analysis or become a part of lab-on-a-chip, the huge conventional reference electrode will be the biggest challenge. For this reason, there are several approaches that have been investigated to solve this problem.

One method to solve this problem is co-fabricated an Ag/AgCl electrode with ISFET, including a gel filled cavity and a porous silicon plug [35]. But this solution has a leakage path from reference electrode to solution that will reduce the device lifetime.

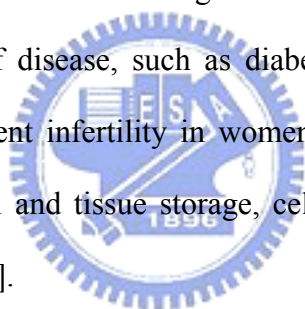
Another method is applying a differential measurement between an ISFET and an identical FET, which does not react on the ion concentration to be measured, called REFET. This method is deposition on top of the ISFET's surface one layer, which is an ion-unblocking membrane that is an insulating polymeric layer exhibiting independence on ionic strength. A commonly used material for ion-unblocking layer in REFET is polyvinylchloride (PVC) [36-37]. The REFET with PVC sensitive membrane has a smaller sensitivity of about 20mV/pH, but it will add some processes to fabricate a REFET and is not compatible with integrated circuit (IC) technology.

The ZrO₂ prepared by dc sputtering process as a pH-sensitive membrane for ISFET is first developed in our laboratory. In this work, we report a simple CMOS compatible REFET by post NH₃ plasma surface treatment on ZrO₂ gate ISFET. The

electrical characteristics and pH response of the ZrO_2 gate ISFET is studied by the standard MOSFET measurement with HP 4156A. Without any unblocking layer to be deposited, the REFET also shows a very low sensitivity of about 28.3 mV/pH. With such ISFET/REFET differential pair, the conventional reference electrode can be replaced by a solid platinum electrode, which can fabricate in the same chip. By this way, a high integration of ISFET with IC fabricating can be realized in the future.

1.4 Applications

There are a wide range of applications for sensors requiring the detection of concentration gradients of metabolites such as oxygen, carbon dioxide, and glucose. Some of the biological applications for sensing the extra cellular gradient of metabolic products include the study of disease, such as diabetes, cancer, and mitochondrial diseases, such as age-dependent infertility in women and Alzheimer's disease, cell and tissue differentiation, cell and tissue storage, cell life cycle and processes, and developmental biology [38-62].



1.5 Outline of the Thesis

In Chapter 1, the ISFET, REFET, ChemFET, and ENFET are briefly described as new ion sensors which represent the combination of the technologies of a MOSFET. It represents a new approach to obtain the chemical characteristics using electrical devices.

In Chapter 2, theories and models of ISFET are described. Such as site-dissociation model, Gouy-Chapman theory, Gouy-Chapman-Stern theory, and drift model are all described here.

In Chapter 3, the zirconium oxide (ZrO_2) membrane has been successfully applied as a pH-sensitive layer for ion-sensitive field-effect transistors (ISFETs). It

exhibited an excellent response range of 56.7~58.3 mV/pH from the fixed current measurement using HP4156A. The ZrO₂ membrane prepared by direct current (DC) sputtering was used as a pH-sensitive film that showed good surface adsorption with oxide and silicon. The pH sensitivities slightly decreased in 1 M NaCl solution; however, the device showed a perfect linear response of 52.5 mV/pH.

In Chapter 4, we used a reference field effective transistor (REFET) to control the effects of temperature and process deviation. After the correction of REFET, we can get a very stable sensitivity and intrinsic drift of SiO₂ gate ISFET and define the thickness of hydration layer that is introduced by the drift effect. According to the result of this study, the thickness of hydration is about 50 nm in SiO₂ membrane ISFET. It exhibits a stable response of 28~32 mV/pH from the fixed current measurement by HP4156A. This method is a really simple way to find the thickness of hydration layer, and it will be useful in the study of the real mechanism in drift effect.

In Chapter 5, a simple and cheap way to solve the drift problem is presented which describes the relation of drift and gate voltage. Constant various gate voltages are biased in sensing layers with reference electrode. It obviously shows a strong relation of gate drifts and gate stress voltages. When the gate voltage is controlled as 0.5 V, the drift voltage of SiO₂ gate ISFET will decrease from 56.12 to 2.94 mV in ten hours measurement. The improvement of drift voltage reaches 94.8%. When the gate voltage is controlled as -1 V, the drift voltage of ZrO₂ gate ISFET will also decrease from -57.94 to 0.76 mV. The improvement of drift voltage reaches 98.7%. This may result from the gate electric field affecting the ions to diffusive into the gate insulator. By this way, we can commercialize the ISFET with a very low drift rate in a simple way.

In Chapter 6, a simple CMOS compatible REFET for pH detection by post NH₃

plasma surface treatment of a ZrO_2 membrane ISFET has been developed. It is a novel study that has latent capacity to integrate the ISFET devices into a chemical micro system for in vivo analysis or become a part of lab-on-a-chip. With the fixed current measurement by HP4156, we can get not only the individual sensitivities of ISFET and REFET, but also the differential sensitivities of ISFET/REFET pair. The ZrO_2 membrane ISFET exhibits an excellent response of 56.7~58.3mV/pH with deviation of 3% and the REFET shows a small response of 27.6~29 mV/pH with a deviation of 5%. Using this ISFET/REFET differential pair, we can get a very stable differential sensitivities of 29.1~29.3 mV/pH with a small deviation of 0.7%. This result indicates that the research not only makes the ISFET integrate into a micro system in a simple way possible, but also increases the stability of sensitivity.

In chapter 7 of the thesis, some conclusions and recommendations of future works are described.



1.6 References

- [1] P. Bergveld, "Development of an ion sensitive solid-state device for neurophysiological measurements," IEEE Trans. Biomed. Eng. vol. 17, pp. 70–71, 1970.
- [2] S. D. Moss, C. C. Johnson, and J. Janata, "Hydrogen calcium and potassium ion sensitive FET transducers," A preliminary report, IEEE Trans. Biomed. Eng. vol. 25 pp. 49–54, 1978.
- [3] H. K. Liao, J. C. Chou, W. Y. Chung, T. P., and S. K. Hsiung, "Study on the interface trap density of the $\text{Si}_3\text{N}_4/\text{SiO}_2$ gate ISFET," Proceedings of the Third East Asian Conference on Chemical Sensors, Seoul, South Korea, pp. 394–400, November 1997.
- [4] L. T. Yin, J. C. Chou, W. Y. Chung, T. P., and S. K. Hsiung, "Study of indium tin oxide thin film for separative extended gate ISFET," Mater. Chem. Phys. vol.70 pp. 12-16, 2001.
- [5] P. Gimmel, B. Gompf, D. Schmeiosser, H. D. Weimhofer, W. Gopel, and M. Klein, " Ta_2O_5 gates of pH sensitive device comparative spectroscopic and electrical studies," Sensors and Actuators B vol. 17 pp. 195–202, 1989.
- [6] J. C. Chou and J. L. Chiang, "Study on the amorphous tungsten trioxide ion-sensitive field effect transistor," Sensors and Actuators B vol. 66 pp. 106-108, 1998.

- [7] T. matsuo and M. Esashi, "Methods of ISFET fabrication" Sens and Actuators vol. 1 pp. 77-96, 1981.
- [8] J. C. Chou and J. L. Chiang, "Ion sensitive field effect transistor with amorphous tungsten trioxide gate for pH sensing" Sens and Actuators B vol. 62 pp. 81-87 2000.
- [9] K. M. Chang, K. Y. Chao, T. W. Chou, and C. T. Chang, "Characteristics of Zirconium Oxide Gate Ion-sensitive Field-Effect Transistors" Japanese Journal of Applied Physics vol. 46 No. 7A pp. 4334-4338, 2007.
- [10] A. G. Revesz, "On the mechanism of the ion sensitive field effect transistors," Thin Solid Films vol. 41, pp. 643–647, 1997.
- [11] P. Bergveld, N. F. de Rooij, and J. N. Zemel, "Physical mechanisms for chemically sensitive semiconductor devices," Nature vol. 273, pp. 438–443, 1978.
- [12] W. M. Siu and R. S. C. Cobbold, "Basic properties of the electrolyte-SiO₂-Si system: physical and theoretical aspects," IEEE Trans. Electron Devices ED vol. 26 , pp. 1805–1815, 1979.
- [13] L. Bousse, N.F. de Rooij and P. Bergveld, "Operation of chemically sensitive field-effect sensor as a function of the insulator–electrolyte interface," IEEE Trans. Electron Devices ED vol. 30 , pp. 1263–1270, 1983.
- [14] A. van den Berg, P. Bergveld, D. N. Reinhondt, and E. J. R. Sudholten, "Sensitivity control of ISFETs by chemical surface modification," Sens. Actuators vol. 8 , pp. 129–148, 1985.
- [15] C. D. Fung, P. W. Cheung, and W. H. Ko, "A generalized theory of an electrolyte–insulator–semiconductor field-effect transistor," IEEE Trans.

- Electron Devices ED vol. 33, pp. 8–18, 1986.
- [16] R. E. G. van Hal, J. C. T. Eijkel, and P. Bergveld, “A novel description of ISFET sensitivity with buffer capacity and double-layer capacitance as key parameters,” *Sens. Actuators B* vol. 24–25, pp. 201–205, 1995.
- [17] G. Massobrio, M. Grattarola, G. Mattioli, and F. Mattioli, Jr., “ISFET-based bio-sensor modeling with SPICE,” *Sens. Actuators B* vol. 1, pp. 401–407, 1990.
- [18] S. Martinoia, G. Massobrio, and M. Grattarola, “An ISFET model for CAD applications,” *Sens. Actuators B* vol. 8, pp. 261–265, 1992.
- [19] M. Grattarola, G. Massobrio, and S. Martinoia, “Modeling H^+ -sensitive FETs with SPICE. IEEE Trans,” *Electron Devices, ED* vol. 39, pp. 813–819, 1992.
- [20] G. Massobrio, S. Martinoia, and M. Grattarola, “Use of SPICE for modeling silicon-based chemical sensors,” *Sens. Mater.* vol. 62, pp. 101–123, 1994.
- [21] S. Martinoia and G. Massobrio, “A behavioral macromodel of the ISFET in SPICE,” *Sens. Actuators B* vol. 62, pp. 182–189, 2000.
- [22] C. W. Mundt and H. T. Nagle, “Applications of SPICE for modeling miniaturized biomedical sensor systems,” *IEEE Trans. Biomed. Eng. BME* vol. 47, pp. 149–154, 2000.
- [23] B. Palan, F. V. Santos, J. M. Karam, B. Courtois, and M. Husak, “New ISFET sensor interface circuit for biomedical applications,” *Sens. Actuators B* vol. 57, pp. 63–68, 1999.
- [24] S. Ingebrandt, C. K. Yeung, W. Staab, T. Zetterer, and A. Offenhausser, “Backside contacted field effect transistor array for extracellular signal recording,” *Biosens. Bioelectron.* vol. 18, pp. 429–435, 2003.
- [25] M. Albareda-Sirvent, A. Merkoci, and S. Alegret, “Thick-film bio-sensors for pesticides produced by screen-printing of graphite–epoxy composite and biocomposite pastes,” *Sens. Actuators B* vol. 79, pp. 48–57, 2001.

- [26] S. J. Birrell and J. W. Hummel, "Real-time multi ISFET/FIA soil analysis system with automatic sample extraction." *Comput. Electron. Agric.* vol. 32, pp. 45–67, 2001.
- [27] J. Artigas, A. Beltran, C. Jimenez, J. Bartroli, and J. Alonso, "Development of a photopolymerisable membrane for calcium ion sensors. Applications to soil drainage waters." *Anal. Chim. Acta* vol. 426, pp. 3–10, 2001.
- [28] A. Poghossian, A. Baade, H. Emons, and M. J. Schoning, "Application of ISFET for pH measurements in rain droplets," *Sens. Actuators B* vol. 76, pp. 634–638, 2001.
- [29] J. Artigas, C. Jimenez, C. Dominguez, S. Minguéz, A. Gonzalo, and J. Alonso, "Development of a multiparametric analyser based on ISFET sensors applied to process control in the wine industry," *Sens. Actuators B* vol. 89, pp. 199–204, 2003.
- [30] P. Bergveld and A. Sibbald, "Analytical and Biomedical Applications of ISFETs," Elsevier, Amsterdam, Netherlands, 1988.
- [31] A. J. Cunningham, "Introduction to Bioanalytical Sensors," Wiley Interscience, 1998.
- [32] U.E. Spichiger-Keller, "Chemical Sensors and Biosensors for Medical and Biological Applications," Wiley, New York, 1998.
- [33] U. Bilitewski and A. Turner (Eds.), "Biosensors in Environmental Monitoring," Taylor & Francis, London, Philadelphia, 2000.
- [34] M. Grattarola, G. Massobrio, *Bioelectronics Handbook*, "Mosfets, Biosensors, and Neurons," McGraw-Hill, New York, USA, 1998.
- [35] R. L. Smith and D. C. Scott, "An integrated sensor for electrochemical

- measurements,” *IEEE Trans. Biomed. Eng. BME* vol. 33 pp. 83-90, 1986.
- [36] M. Chudy, W. Wroblewski, and Z. Brzozka, “Towards REFET,” *Sensors and Actuators B* vol. 57 pp. 47-50, 1999.
- [37] P. A. Hammond, D.R.S. Cumming, and D. Ali, “A single-Chip pH Sensor Fabricated by a Conventional CMOS Process,” *Proceeding of IEEE Sensors* vol. 1 pp. 350-355, 2002.
- [38] M. J. Muehlbauer, E. J. Guilbeau, B. C. Towe, and T. A. Brandon, “Thermoelectric enzyme sensor for measuring blood glucose,” *Biosens. Bioelectron.*, vol. 5, pp. 1–12, 1990.
- [39] W. J. Whalen, “Some problems with an intracellular pO electrode,” *Adv. Exp. Med. Biol.*, vol. 50, pp. 39–41, 1974.
- [40] R. T. Kennedy, L.M. Kauri, G. M. Dahlgren, and S.-K. Jung, “Metabolic oscillations in beta-cells,” *Diabetes*, vol. 51, pp. S152–S161, 2002.
- [41] S. K. Jung, W. Gorski, G. A. Aspinwall, L. M. Kauri, and R. T. Kennedy, “Oxygen microsensor and its application to single cells and mouse pancreatic islets,” *Anal. Chem.*, vol. 71, pp. 3642–3649, 1999.
- [42] Q. Zhang, P. Wang, J. Li, and X. Gao, “Diagnosis of diabetes by image detection of breath using gas-sensitive LAPS,” *Biosens. Bioelectron.*, vol. 15, pp. 249–256, 2000.
- [43] D. L. Keefe, “Aging and infertility in women,” *Med. Health*, vol. 80, pp. 403–405, 1997.
- [44] N. R. Sims, “Energy metabolism, oxidative stress and neuronal degeneration in Alzheimer’s disease,” *Neurodegeneration*, vol. 5, pp. 435–440, 1996.
- [45] Y.-S. Torisawa, T. Kaya, Y. Takii, D. Oyamatus, M. Nishizawa, and T. Matsue, “Scanning electrochemical microscopy-based drug sensitivity test for a cell

- culture integrated in silicon microstructures,” *Anal. Chem.*, vol. 75, pp. 2154–2158, 2003.
- [46] D. E. Woolley, L. C. Tetlow, D. J. Adlam, D. Gearey, R. D. Eden, T. H. Ward, and T. D. Allen, “Electrochemical monitoring of anticancer compounds on the human ovarian carcinoma cell line A2780 and its adriamycin- and cisplatin-resistant variants,” *Exp. Cell Res.*, vol. 273, pp. 65–72, 2002.
- [47] B. Liu, S. A. Rotenberg, and M. V. Mirkin, “Scanning electrochemical microscopy of living cells: different redox activities of nonmetastatic and metastatic human breast cells,” in *PNAS*, vol. 97, pp. 9855–9860, 2000.
- [48] B. Liu, W. Cheng, S. A. Rotenberg, and M. V. Mirkin, “Scanning electrochemical microscopy of living cells part 2. Imaging redox and acid/basic reactivities,” *J. Electroanal. Chem.*, vol. 500, pp. 590–597, 2001.
- [49] W. Feng, S. A. Rotenberg, and M. V. Mirkin, “Scanning electrochemical microscopy of living cells. 5. Imaging of fields of normal and metastatic human breast cells,” *Anal. Chem.*, vol. 75, pp. 4148–4154, 2003.
- [50] C. Cai, B. Liu, and M. V. Mirkin, “Scanning electrochemical microscopy of living cells. 3. *Rhodobactersphaeroides*,” *Anal. Chem.*, vol. 74, pp. 114–119, 2002.
- [51] B. D. Bath, E. R. Scott, J. B. Phipps, and H. S. White, “Scanning electrochemical microscopy of iontophoretic transport in hairless mouse skin. Analysis of the relative contributions of diffusion, migration, and electroosmosis to transport in hair follicles,” *J. Pharm. Sci.*, vol. 89, pp. 1537–1549, 2000.
- [52] E. R. Scott and H. S. White, “Iontophoretic transport through porous membranes using scanning electrochemical microscopy: application to in vitro studies of ion fluxes through skin,” *Anal. Chem.*, vol. 65, pp. 1537–1545, 1993.
- [53] L. Csonge, D. Bravo, H. Newman-Gage, T. Rigley, E. U. Conrad, A. Bakay, D. M. Strong, and S. Pellet, “Banking of osteochondral allografts, part II.

- Preservation of chondrocyte viability during long-term storage,” *Cell and Tissue Banking*, vol. 3, pp. 161–168, 2002.
- [54] D. R. Ambruso, D. Mitchell, S. Karakoleva, S. Lavery, J. Otis, T. Danielson, and J. Mladenovic, “Comparison of room temperature (RT) or 4 C storage of cord blood before processing: recovery after freezing,” in 44th Annu. Meeting Amer. Soc. Hematology, Philadelphia, PA, Dec., 6–10 2002.
- [55] P. D. Ribotta, A. E. Leon, and M. C. Anon, “Effects of yeast freezing in frozen dough,” *Cereal Chem.*, vol. 80, pp. 454–458, 2003.
- [56] S. L. Holliday and L. R. Beuchat, “Viability of *Salmonella*, *Escherichia coli* 0157:H7, and *Listeria monocytogenes* in yellow fat spreads as affected by storage temperature,” *J. Food Protection*, vol. 66, pp. 549–558, 2003.
- [57] N. Mansour, F. Lahnsteiner, and B. Berger, “Metabolism of intratesticular spermatozoa of a tropical teleost fish (*Clarias gariepinus*),” *Comp. Biochem. Physiol. B: Biochem. Mol. Biol.*, vol. 135B, pp. 285–296, 2003.
- [58] C. E. Helmstetter, M. Thornton, and N. B. Grover, “Cell-cycle research with synchronous cultures: an evaluation,” *Biochimie*, vol. 83, pp. 83–89, 2001.
- [59] S. Umehara, Y. Wakamoto, I. Inoue, and K. Yasuda, “On-chip single-cell microcultivation assay for monitoring environmental effects on isolated cells,” *Biochem. Biophys. Res. Comm.*, vol. 305, pp. 534–540, 1993.
- [60] P. J. S. Smith and P. G. Haydon, A. Hengstenberg, and S.-K. Jung, “Analysis of cellular boundary layers: application of electrochemical microsensors,” *Electrochim. Acta*, vol. 47, pp. 283–292, 2001.
- [61] H. Shiku, T. Shiraishi, H. Ohya, T. Matsue, H. Abe, H. Hoshi, and M. Kobayashi, “Oxygen consumption of single bovine embryos probed by scanning electrochemical microscopy,” *Anal. Chem.*, vol. 73, pp. 3751–3758, 2001.

Chapter 2

Theory

2.1 ISFET's Model

It is not difficult to find out the similarities between ISFET and MOSFET. The most obvious characteristics are the similarity between their structures. Therefore, the best way to comprehend the ISFET is to understand the operating principle of a MOSFET first. When MOSFET is operated in the so-called linear region, the drain current I_D is given by

$$I_D = \frac{C_{OX}\mu W}{L} \left\{ (V_{GS} - V_T) - \frac{1}{2}V_{DS} \right\} V_{DS} \quad (1)$$

where C_{OX} is the gate insulator capacitance per unit area, μ the electron mobility in the channel and W/L the width-to-length ratio of the channel.

The threshold voltage V_T of Eq. (1) is described by the following expression:

$$V_T = V_{FB} - \frac{Q_B}{C_{OX}} + 2\phi_F \quad (2)$$

where V_{FB} is the flat-band voltage, Q_B is the depletion charge in the substrate, and ϕ_F is the potential difference between the Fermi levels of doped and intrinsic silicon. For a MOSFET with charges presence in the oxide and at the oxide-semiconductor interface, the flat-band voltage can be given by

$$V_{FB} = \frac{\Phi_M - \Phi_{Si}}{q} - \frac{Q_{OX} + Q_{SS}}{C_{OX}} \quad (3)$$

where Φ_M is the work function of the gate metal, Φ_{Si} is the work function of silicon, Q_{OX} is the charge in the oxide and Q_{SS} is the surface state density at the oxide-silicon interface. Substitution of Eq. (3) into Eq. (2), the general form of the threshold voltage of a MOSFET becomes

$$V_T = \frac{\Phi_M - \Phi_{Si}}{q} - \frac{Q_{OX} + Q_{SS} + Q_B}{C_{OX}} + 2\phi_F \quad (4)$$

This equation holds for the MOSFET. But in case of the ISFET, the metal gate is

no longer present, so that the term Φ_M/q must be revised. Figure 2-1 illustrates the similarities and differences between these two devices. It can be seen that the reference electrode, the aqueous solution and the phenomena occurring at the oxide-solution interface must be accounted for instead of Φ_M/q . Bergved and Sibbald [1] showed that the threshold voltage for the ISFET becomes

$$V_T = E_{ref} + \chi^{sol} - \Psi_0 - \frac{\Phi_{Si}}{q} - \frac{Q_{OX} + Q_{SS} + Q_B}{C_{OX}} + 2\phi_F \quad (5)$$

where E_{ref} represents the constant potential of the reference electrode, χ^{sol} is the surface dipole potential of the solution which also has a constant value. The term Ψ_0 representing the surface potential at the oxide-electrolyte interface is the key element that makes ISFET pH-sensitive.

The surface of any metal oxide always contains hydroxyl groups, in the case of silicon dioxide SiOH groups. These groups can be protonated and deprotonated, and thus, when the gate oxide contacts an aqueous solution, a change of pH will change the SiO₂ surface potential. These reactions can be expressed by [2]



where H_S^+ represents the protons at the surface of the oxide, K_1 and K_2 are the dissociation constants of these two chemical equations.

The potential between electrolyte solution and insulator surface causes a proton concentration difference between the bulk and surface (Fig. 2-2) that is according to Boltzmann [3]

$$a_{H_S^+} = a_{H_B^+} \exp \frac{-q\Psi_0}{kT} \quad (8)$$

where k is the Boltzmann constant, T is the absolute temperature, $a_{H_S^+}$ and $a_{H_B^+}$ are the activities of H_S^+ at the oxide surface and in the solution bulk, respectively.

According to the definition of pH, Eq. (8) can be expressed by

$$pH_S = pH_B + \frac{q\Psi_0}{2.3kT} \quad (9)$$

where pH_S is the pH value at the oxide surface, pH_B is the pH value in the solution bulk.

The pH response, which is generally called the sensitivity, is defined as the surface potential change over a pH unit change. This response is given by [4]

$$\frac{\delta\Psi_0}{\delta pH_B} = -2.3 \frac{kT}{q} \alpha \quad (10)$$

with

$$\alpha = \frac{1}{\frac{2.3kTC_{dif}}{q^2\beta_{int}} + 1} \quad (11)$$

where C_{dif} is the differential capacitance, and β_{int} is the intrinsic buffer capacity. α is a dimensionless sensitivity parameter. The value of α varies between 0 and 1 depending on the intrinsic buffer capacity and the differential capacitance. If α equals 1, the theoretical maximum sensitivity of -59.2 mV/pH at room temperature can be obtained. Eq. (10) and eq. 11) show that the parameter of α plays an important role of the sensitivity. And the value of α is depend on the relation of C_{dif} and β_{int} . There are several approaches in colloid chemistry to describe C_{dif} and β_{int} . Some models will describe as follows.

2.2 The Site-Dissociation Model

There are a lot of inorganic insulators [5-12] which are used for ISFET process technology. The site-dissociation model introduced by Yate et al. [2] is used to drive the intrinsic buffer capacity for these inorganic membranes. This model describes the charges between oxide and electrolyte. The basic assumed is that the surface sites act as discrete sites for chemical reactions at the surface when it is brought in contact

with an electrolyte solution. General speaking, there is only a single type of site to be present with an amphoteric character for the inorganic oxides. That means that each surface site can be neutral, act as a proton donor or act as a proton acceptor. Figure 2-3 shows the surface property of site-dissociation model, where A represents the central atom of oxide molecular. Fundamentally, this can describe the appropriate acidic and basic reactions between the A-OH sites at the surface and the H⁺ ions in the bulk solution. From the corresponding thermodynamic equilibrium equations, one can calculate the relationship between the interfacial equilibrium potential ψ_0 and the H⁺ ion concentration in the bulk of the solution, [H⁺]_b, or , in other words, the relationship between ψ_0 and pH.

The most commonly used description, however, is based on the equilibrium between the surface OH groups and the H⁺ ions located directly near the surface, denoted as H_s⁺. The acidic and basic characters of the neutral site A-OH are characterized by the equilibrium constants K_a and K_b, respectively. The equations can be written as follows:



with:

$$K_a = \frac{[AO^-][H^+]_s}{[AOH]} \quad (14)$$

$$K_b = \frac{[AOH_2^+]}{[AOH][H^+]_s} \quad (15)$$

where s means the surface.

From above reactions, we can get the following thermodynamic equations:

$$\mu_{AOH}^0 + kT \ln v_{AOH} = \mu_{AO^-}^0 + kT \ln v_{AO^-} + \mu_{H_s^+}^0 + kT \ln \alpha_{H_s^+} \quad (16)$$

and

$$\mu_{AOH_2^+}^0 + kT \ln v_{AOH_2^+} = \mu_{AOH}^0 + kT \ln v_{AOH} + \mu_{H_3^+}^0 + kT \ln \alpha_{H_3^+} \quad (17)$$

where v_i is the surface activity and μ_i^0 is the standard chemical potential of species i .

Equations (3) and (4) can be rewritten as follows:

$$\frac{v_{AO^-} a_{H_3^+}}{v_{AOH}} = K_a \quad \text{with} \quad K_a = \exp \frac{\mu_{AOH}^0 - \mu_{AO^-}^0 - \mu_{H_3^+}^0}{kT} \quad (18)$$

$$\frac{v_{AOH} a_{H_3^+}}{v_{AOH_2^+}} = K_b \quad \text{with} \quad K_b = \exp \frac{\mu_{AOH_2^+}^0 - \mu_{AOH}^0 - \mu_{H_3^+}^0}{kT} \quad (19)$$

where the K values are dimensionless intrinsic dissociation constants. The K values are real constants independent of the ionization state of the oxide surface. When the Boltzmann equation is applied, the surface charge density, σ_0 , can be given as follows:

$$\sigma_0 = q(v_{AOH_2^+} - v_{AO^-}) = qN_s(\Theta^+ - \Theta^-) \quad (20)$$

where N_s is the density of the available sites; Θ^+ and Θ^- are the fractions AOH_2^+ and AO^- of N_s , respectively. The fractions Θ^+ and Θ^- can be calculated by Eqs (1) and (2), and substituted in (20) to give:

$$\sigma_0 = qN_s \left(\frac{a_{H_3^+}^2 - K_a K_b}{K_a K_b + K_b a_{H_3^+} + a_{H_3^+}^2} \right) = -q[B] \quad (21)$$

Taking the pH variations in the interface of oxide and electrolyte into account, the surface charge density versus the β_{int} pH variation on the surface can be calculated as following definition:

$$\frac{\delta \sigma_0}{\delta pH_s} = -q \frac{\delta[B]}{\delta pH_s} = -q \beta_{\text{int}} \quad (22)$$

where β_{int} is called the intrinsic buffer capacity, depending on the activity of surface H^+ -ions.

And thus we can finally find the expression for the intrinsic buffer capacity:

$$\beta_{\text{int}} = N_s \frac{K_b a_{H_3^+}^2 + 4K_a K_b a_{H_3^+} + K_a K_b^2}{(K_a K_b + K_b a_{H_3^+} + a_{H_3^+}^2)^2} 2.3 a_{H_3^+} \quad (23)$$

2.3 The Gouy-Chapman Theory

According to the charge neutrality, an equal but opposite charge is built up, σ_{DL} , in the electrolyte solution side of the double layer. Thus there will be, something like capacitor (Figure 2-2), built up in the oxide/electrolyte system. We can obtain the following Eq. by such equilibrium in Boltzmann equation:

$$c_i(x) = c_i^0 \exp\left(\frac{-z_i q \phi_x}{kT}\right) \quad (24)$$

where ϕ_x is the potential at any distance x with respect to the bulk of the solution; $c_i(x)$ and c_i^0 are the molar concentrations of species i at a distance x and in the bulk of the solution respectively and z_i is the magnitude of the charge on the ions. The combination of the Boltzmann and the Poisson equation, which relates the charge density with the potential, is obtained as follows:

$$\sigma_{DL} = -(8kT \varepsilon \varepsilon_0 n^0)^{\frac{1}{2}} \sinh\left(\frac{zq\psi_0}{2kT}\right) = -C_0 \psi_0 = -\sigma_0 \quad (25)$$

where ε_0 is the permittivity of free space and ε is the relative permittivity; n^0 is the number concentration of each ion in the bulk. Differentiation of Eq.(25) with respect ψ_0 and rearrangement gives the following expression for the differential capacitance:

$$C_{dif} = \left(\frac{2\varepsilon\varepsilon_0 z^2 q^2 n^0}{kT}\right)^{\frac{1}{2}} \cosh\left(\frac{zq\psi_0}{2kT}\right) \quad (26)$$

The Gouy-Chapman theory has one drawback. The ions are considered as point charges that can approach the surface arbitrarily close. The assumption causes unrealistic high concentrations of ions near the surface at high values of ψ_0 . an adjustment to solve this problem was first suggested by stern and is described in the next section.

2.4 The Gouy-Chapman-Stern Theory

The Gouy-Chapman-Stern model involves a diffuse layer of charge in the solution

starting at a distance x_2 from the surface. The charge in the diffuse layer is [13]:

$$\sigma_{DL} = -(8kT \varepsilon \varepsilon_0 n^0)^{\frac{1}{2}} \sinh\left(\frac{zq\phi_2}{2kT}\right) = -C_0 \psi_0 = -\sigma_0 \quad (27)$$

where ϕ_2 is the potential at any distance x_2 . Differentiating and rearranging (27) gives the following expression for the differential capacitance:

$$C_{dif} = \frac{\left(\frac{2\varepsilon\varepsilon_0 z^2 q^2 n^0}{kT}\right)^{\frac{1}{2}} \cosh\left(\frac{zq\phi_2}{2kT}\right)}{1 + \left(\frac{x_2}{\varepsilon\varepsilon_0}\right) \left(\frac{2\varepsilon\varepsilon_0 z^2 q^2 n^0}{kT}\right)^{\frac{1}{2}} \cosh\left(\frac{zq\phi_2}{2kT}\right)} \quad (28)$$

To simplify the above equation as follows

$$\frac{1}{C_{dif}} = \frac{x_2}{\varepsilon\varepsilon_0} + \frac{1}{\left(\frac{2\varepsilon\varepsilon_0 z^2 q^2 n^0}{kT}\right)^{\frac{1}{2}} \cosh\left(\frac{zq\phi_2}{2kT}\right)} \quad (29)$$

There will be seen easily, the differential capacitance can be distinguish into two parts, the first term is the contribution of the called diffuse layer, and the second term is the contribution of the Stern layer. Then the following equation will be obtained:

$$\psi_0 = \frac{\sigma_0}{C_{i,d}} + \frac{\sigma_0}{C_{i,st}} = \phi_2 + \frac{(8kT \varepsilon \varepsilon_0 n^0)^{\frac{1}{2}} \sinh\left(\frac{zq\phi_2}{2kT}\right)}{C_{i,st}} \quad (30)$$

2.5 Site-Dissociation and Gouy-Chapman-Stern Model

The combination of the site-dissociation model with Gouy-Chapman-Stern model is probably the most widely used combination to describe the oxide/electrolyte solution interface. Dzombak and Morel used the site-dissociation model in combination with the Gury-Chapman model to describe the surface complication of hydrous ferric oxide [14]. The relation between the parameters $a_{H_s^+}$ and ψ_0 can be derived by solving (21) and (25) to obtain:

$$a_{H_s^+} = \frac{K_b C_i \psi_0 + \sqrt{(K_b C_i \psi_0)^2 - 4K_a K_b (q^2 N_s^2 - C_i^2 \psi_0^2)}}{2(qN_s - C_i \psi_0)} \quad (31)$$

This relation is necessary to link the calculated intrinsic buffer capacity and the differential capacitance.

2.6 Physical Model for Drift

Jamasb firstly proposed the physical model for drift in 1997 [13]. The key point of this model was employing the dispersive transport theory to express the gate voltage drift, which is caused by the hydration effect at the insulator-electrolyte interface. Dispersive transport was briefly reviewed in [15] and it could be characterized by a power-law time decay of the mobility or diffusivity of the form $t^{\beta-1}$, $0 < \beta < 1$. This time dependence is based on a model that interprets transport in terms of a “random walk”. The origin of random walk is either a) hopping motion through localized states giving rise to hopping transport, or b) multiple trapping from a band of extended states or localized states leading to multiple-trap transport. The multiple-trap transport is generally associated with the motion of electrons or holes in disordered materials.

Regardless of the specific dispersive mechanism involved, dispersive transport leads to a characteristic power-law time decay of diffusivity, which can be described by

$$D(t) = D_{00} (\omega_0 t)^{\beta-1} \quad (32)$$

where D_{00} is a temperature-dependent diffusion coefficient which obeys an Arrhenius relationship, ω_0 is the hopping attempt frequency, and β is the dispersion parameter satisfying $0 < \beta < 1$. Dispersive transport leads to decay in the density of sites/traps occupied by the species undergoing transport. This decay is described by the stretched-exponential time dependence given by

$$\Delta N_{S/T}(t) = \Delta N_{S/T}(0) \exp[-(t/\tau)^\beta] \quad (33)$$

where $\Delta N_{ST}(t)$ is the area density (units of cm^{-2}) of sites/traps occupied, τ is the time constant associated with structural relaxation, and β is the dispersion parameter.

Since hydration leads to a change of the chemical composition of the sensing oxide surface, it is reasonable to assume that the dielectric constant of the hydrated surface layer differs from that of the sensing oxide bulk. The overall insulator capacitance, which is determined by the series combination of the surface hydration layer and the underlying oxide, will exhibit a slow, temporal change. When drift phenomenon occurs at the surface of an actively biased ISFET, the gate voltage will simultaneously exhibit a change to keep a constant drain current. The change of the gate voltage can be written as

$$\Delta V_G(t) = V_G(t) - V_G(0) \quad (34)$$

Since the voltage drop inside the semiconductor is kept constant, $\Delta V_G(t)$ becomes

$$\Delta V_G(t) = [V_{FB}(t) - V_{FB}(0)] + [V_{ins}(t) - V_{ins}(0)] \quad (35)$$

where V_{FB} is the flat band voltage and V_{ins} is the voltage drop across the insulator. V_{FB} and V_{ins} are given by

$$V_{FB} = E_{ref} + \chi^{sol} - \Psi_0 - \frac{\Phi_{Si}}{q} - \frac{Q_{OX} + Q_{SS}}{C_{OX}} \quad (36)$$

$$V_{ins} = \frac{-(Q_B + Q_{inv})}{C_{OX}} \quad (37)$$

where Q_{inv} is the inversion charge. If the temperature, pH, and the ionic strength of the solution are held constant, E_{ref} , χ^{sol} , Ψ_0 , and Φ_{Si} can be neglected, so the drift can be rewritten as

$$\Delta V_G(t) = -(Q_{OX} + Q_{SS} + Q_B + Q_{inv}) \left[\frac{1}{C_i(t)} - \frac{1}{C_i(0)} \right] \quad (38)$$

In this study, the gate oxide of the fabricated ISFET was composed of two layers, a

lower layer of thermally-grown SiO₂ of thickness, x_L , and upper layer of PECVD SiO₂ of thickness, x_U . $C_I(0)$ is the effective insulator capacitance given by the series combination of the thermally-grown SiO₂ capacitance, ε_L/x_L , and the PECVD SiO₂ capacitance, ε_U/x_U . $C_I(t)$ is analogous to $C_I(0)$, but an additional hydrated layer of capacitance, ε_{HL}/x_{HL} , at the oxide-electrolyte interface must be taken into consideration, and the PECVD SiO₂ capacitance is now given by $\varepsilon_U/[x_U - x_{HL}]$. The series combinations of the capacitances are illustrated in Figure 2-4. Therefore, the drift is given by

$$\Delta V_G(t) = -(Q_{OX} + Q_{SS} + Q_B + Q_{inv}) \left(\frac{\varepsilon_U - \varepsilon_{HL}}{\varepsilon_U \varepsilon_{HL}} \right) x_{HL}(t) \quad (39)$$

From this equation, we observed that drift is directly proportional to the thickness of the hydrated layer. By applying dispersive transport theory, an expression for $x_{HL}(t)$ is given by [16]

$$x_{HL}(t) = x_{HL}(\infty) \left\{ 1 - \exp[-(t/\tau)^\beta] \right\} \quad (40)$$

with

$$x_{HL}(\infty) = \frac{D_{00} \omega_0^{\beta-1} \Delta N_{S/T}(0)}{A_D \beta N_{hydr}} \quad (41)$$

where A_D represents the cross-sectional area, and N_{hydr} is the average density of the hydrating species per unit volume of hydration layer. Thus, the overall expression for the gate voltage drift is

$$\Delta V_G(t) = -(Q_{OX} + Q_{SS} + Q_B + Q_{inv}) \left(\frac{\varepsilon_U - \varepsilon_{HL}}{\varepsilon_U \varepsilon_{HL}} \right) x_{HL}(\infty) \left\{ 1 - \exp[-(t/\tau)^\beta] \right\} \quad (42)$$

From this equation, we can expect that if the time of gate oxide immersing in the

test-solution is long enough that is in a stable state (determined by the constant τ), the gate voltage drift will approach a constant value which is greatly dependent on the hydration depth.

$$\Delta V_G(t) \doteq x_{HL}(t) \doteq x_{HL}(\infty) \quad (43)$$

Then we can determinate the hydration depth of the oxide layer.



2.7 References

- [1] P. Bergveld, "Thirty years of ISFETOLOGY What happened in the past 30 years and what may happen in the next 30 years," *Sens. Actuators B* vol. 88, pp. 1-20, 2003
- [2] D. E. Yates, S. Levine, and T. W. Healy, "Site-binding model of the electrical double layer at the oxide/water interface," *J. Chem. Soc. Faraday Trans. I* vol. 70 pp.1807-1844, 1974.
- [3] W. M. Siu and R. S. C. Cobbold,"Basic Properties of the Electrolyte-SiO₂-Si System:Physical and Theoretical Aspects," *IEEE Trans. Electron Devices*, ED vol. 26, pp. 1805-1815, 1979.
- [4] S. Jamasb, S. Collins, and R.L. Smith, A physically-based model for drift in Al₂O₃-gate pH ISFET's, *Tech. Digest, 9th Int. Conf. Solid-State Sensors and Actuators (Transducers '97)*, Chicago, IL, 15-19, pp. 1379-1382, June, 1997.
- [5] S. D. Moss, C. C. Johnson, and J. Janata, "Hydrogen calcium and potassium ion sensitive FET transducers," A preliminary report, *IEEE Trans. Biomed. Eng.* vol. 25 pp. 49-54, 1978.
- [6] H. K. Liao, J. C. Chou, W. Y. Chung, T. P., and S. K. Hsiung, "Study on the interface trap density of the Si₃N₄/SiO₂ gate ISFET," *Proceedings of the Third East Asian Conference on Chemical Sensors*, Seoul, South Korea, pp. 394-400, November 1997.
- [7] L. T. Yin, J. C. Chou, W. Y. Chung, T. P., and S. K. Hsiung, "Study of indium tin oxide thin film for separative extended gate ISFET," *Mater. Chem. Phys.* vol.70 pp. 12-16, 2001.
- [8] P. Gimmel, B. Gompf, D. Schmeiosser, H. D. Weimhofer, W. Gopel, and M.

- Klein, "Ta₂O₅ gates of pH sensitive device comparative spectroscopic and electrical studies," *Sensors and Actuators B* vol. 17 pp. 195–202, 1989.
- [9] J. C. Chou and J. L. Chiang, "Study on the amorphous tungsten trioxide ion-sensitive field effect transistor," *Sensors and Actuators B* vol. 66 pp. 106-108, 1998.
- [10] T. matsuo and M. Esashi, "Methods of ISFET fabrication" *Sens and Actuators* vol. 1 pp. 77-96, 1981.
- [11] J. C. Chou and J. L. Chiang, "Ion sensitive field effect transistor with amorphous tungsten trioxide gate for pH sensing," *Sens and Actuators B* 62 pp. 81-87, 2000.
- [12] K. M. Chang, K. Y. Chao, T. W. Chou, and C. T. Chang, "Characteristics of Zirconium Oxide Gate Ion-sensitive Field-Effect Transistors" *Japanese Journal of Applied Physics* Vol. 46 No. 7A pp. 4334-4338, 2007.
- [13] A. J. Bard and Faulkner, *Electrochemical methods fundamentals and applications*. John Wiley & Sons, New York, 1980.
- [14] D. A. dzombak and F. M. M. Morel, "Surface complexation modeling," *Hydrous Ferric Oxide*. John Wiley & Sons, New York, 1990.
- [15] S. Jamasb, S.D. Collins and R.L. Smith, "A physical model for threshold voltage instability in Si₃N₄-gate H⁺-sensitive FET's (pH ISFET's)," *IEEE Trans. Electron Devices* vol. 45 1239-1245, 1998.
- [16] S. Jamasb, "An analytical technique for counteracting drift in Ion-Selective Field Effect Transistors (ISFETs)," *IEEE Sens. J.* vol. 4, 795-801, 2004.

Table 2- I . Sensitivities and test range for different sensing membranes.

Sensing membrane	Test range (pH)	Sensitivity (mV/pH)	Reference
ZrO₂	1-13	57.5	12
SiO₂	4-10	25-48	10
Si₃N₄	1-13	46-56	6
Al₂O₃	1-13	53-57	4
Ta₂O₅	1-13	56-57	8
SnO₂	2-10	58	6
ITO	2-12	54-58	7
α-WO₃	1-7	50	9
α-Si-H	1-7	50.62	11



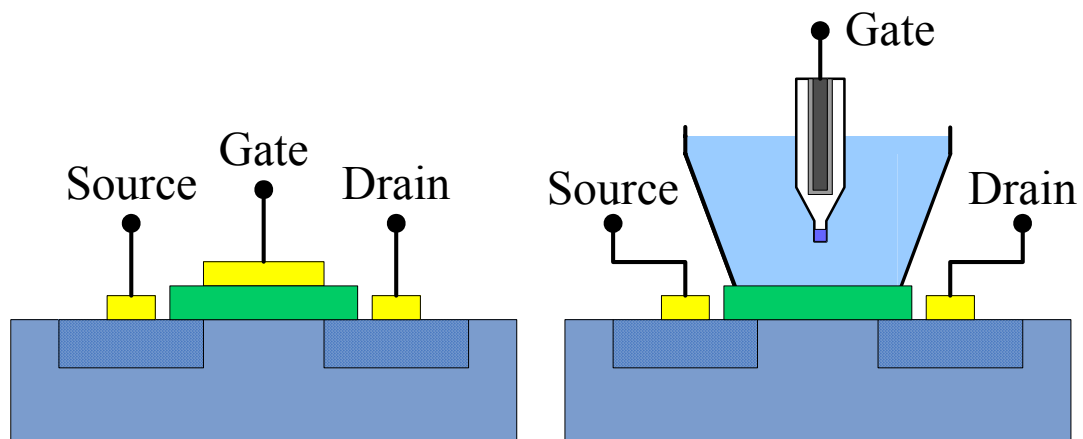


Figure 2-1 The similarities and differences between MOSFET and ISFET devices. It can be seen that the reference electrode, the aqueous solution and the phenomena occurring at the oxide-solution interface must be accounted for instead of Φ_M/q .



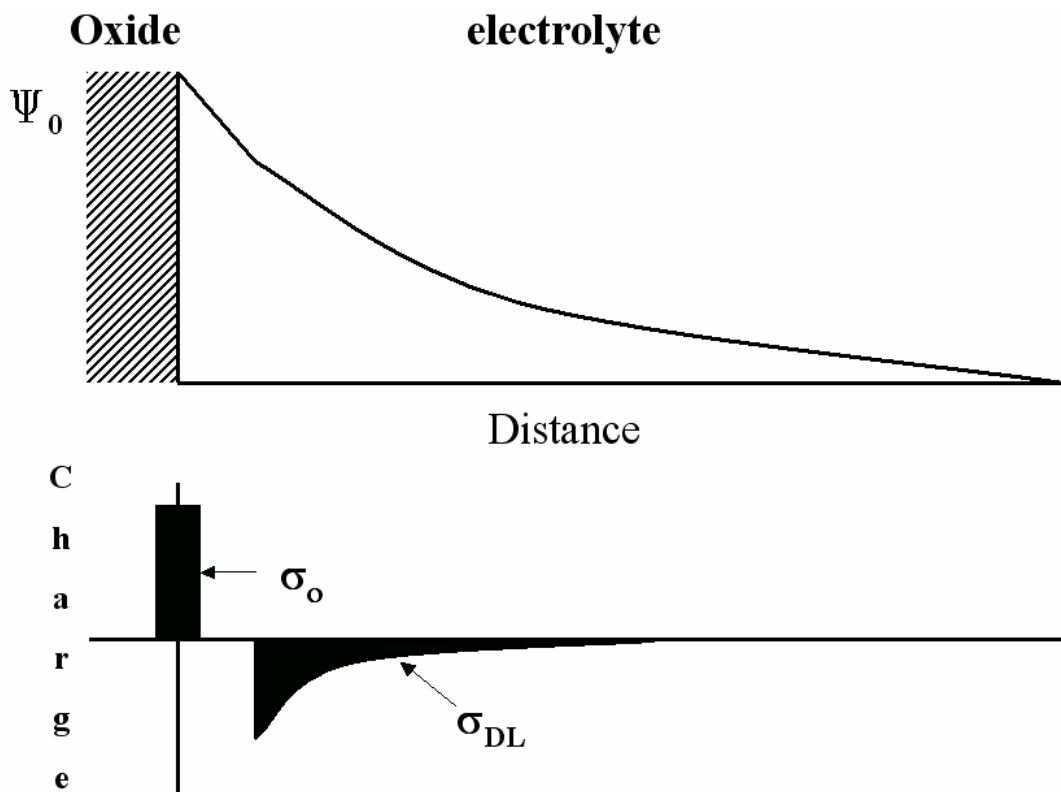


Figure 2-2 Potential profile and charge distribution at an oxide electrolyte solution interface (After Siu et al., Ref. 3).

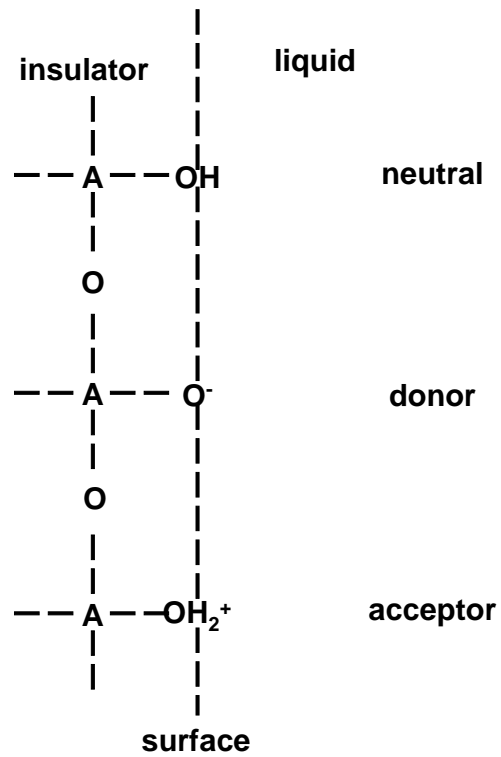
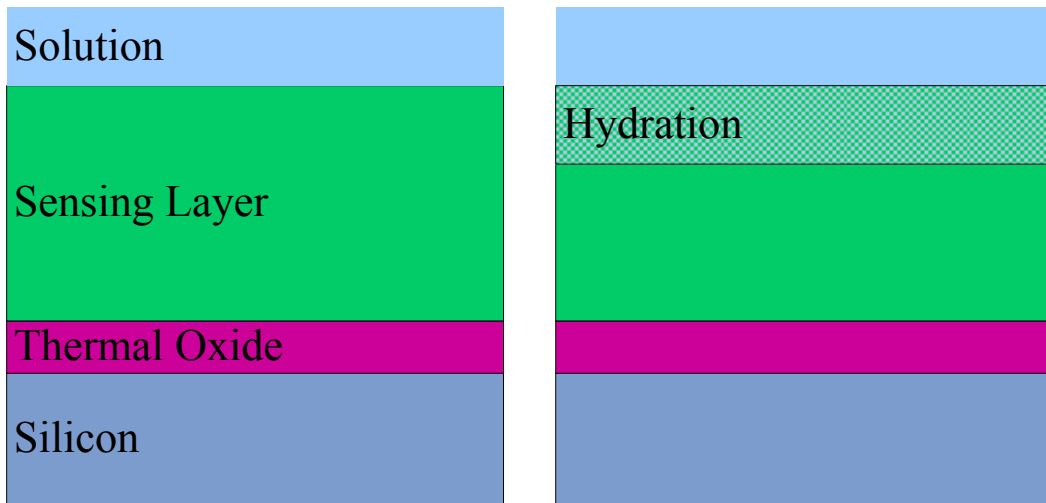


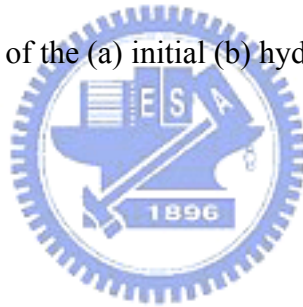
Figure 2-3 Schematic representation of site-dissociation model.



(a)

(b)

Figure 2-4 Series combination of the (a) initial (b) hydrated insulator capacitance.



Chapter 3

Characteristics of Zirconium Oxide (ZrO_2) Gate

Ion-Sensitive Field-Effect Transistors

3.1 Backgrounds and Motivation

Because many chemical and biological processes are dependent on pH, it is one of the most common parameters measured in laboratories. In the past, a glass electrode was usually used for measuring pH until a brainchild technique based on MOSFET called ISFET was demonstrated by Bergveld in 1970 [1]. ISFET is a special type of MOSFET without a metal gate, in which the gate is directly exposed to the buffer solution. When there is a change in the surface potential between the gate insulator and the electrolyte, the electric field at the insulator semiconductor interface will be changed and the channel conductance that affects the drain current will also be modulated. Since the channel conductance and drain current can be modulated, we may measure the changes by applying a fixed source to drain voltage or a constant source to drain voltage current and different output gate voltages. By these methods, we can plot a standard linear line between gate voltages and various pH values, and a standard linear line can be taken to measure an unknown acid or an alkaline solution. Compared with the conventional method, ISFET has some advantages such as small size, short-response time, low cost, and complementary metal-oxide-semiconductor (CMOS) compatible processes. The development of ISFET has been on going for more than 35 years, and the first sensitive membrane used is silicon dioxide (SiO_2), which showed an unstable sensitivity and a large drift. Subsequently, Al_2O_3 , Ta_2O_5 , SnO_2 , TiN, $\alpha\text{-WO}_3$, indium tin oxide (ITO), and ZrO_2 were used as pH-sensitive membranes to achieve a higher pH response and a more stable drift voltage [2~9]. Although ZrO_2 prepared using an electron beam has been used as a sensing film [9],

there are still many characteristics of the ZrO_2 gate ISFET that should be studied, e.g., drift effect or sensitivity in an alkali solution. Table 2-I shows the sensitivities and test ranges of different sensing membranes. We can easily observe that the sensitivity of ZrO_2 prepared by direct current (DC) sputtering is the strongest and has a very wide test range. Thus, a ZrO_2 thin film is very suitable for applications in ISFETs.

In this study, ZrO_2 prepared by DC sputtering as a pH-sensitive membrane for ISFET was first developed in our laboratory. The electrical characteristics and pH response of the ZrO_2 gate ISFET were studied by standard MOSFET measurement using HP4156A. Drift voltage was also calculated by drain current-to-gate voltage (I_D - V_G) measurement.

3.2 Experimental Procedure

3.2.1 Device Fabrication

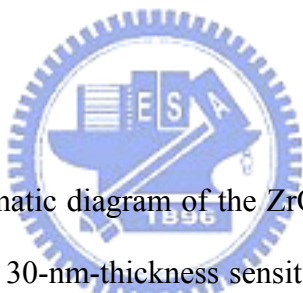


Figure 3-1 shows a schematic diagram of the ZrO_2 gate ISFET that is fabricated by the MOSFET technique. A 30-nm-thickness sensitive layer of the ZrO_2 membrane was deposited onto the SiO_2 gate ISFET by DC sputtering with 4 in. diameter and 99.99% purity of Zr in oxygen atmosphere. The total sputtering pressure was 20 mTorr in the mixed gases Ar and O_2 for 200 minutes while the base pressure was 3×10^{-6} Torr, and the RF power was 200 W and the operating frequency was 13.56MHz. Table II shows the detailed growth conditions for film deposition using the sputtering system. After post annealing at $600^\circ C$, the ZrO_2 membrane is defined using photoresist and etched by buffer oxide etch (BOE). The ISFETs were fabricated on a p-type silicon wafer with (100) orientation and the manufacturing processes are as follows:

- (1) RCA cleaning of 4 in. p-type silicon wafer
- (2) Wet oxidation of silicon dioxide (600 nm)

- (3) Defining of S/D area with mask I and wet etching of silicon dioxide by BOE
- (4) Thermal growth of silicon dioxide as screen oxide (30 nm)
- (5) Phosphorus ion implantation and post annealing at 950°C
- (6) PECVD of silicon dioxide for passivation layer
- (7) Defining of contact hole and gate region with mask II and wet etching of silicon dioxide by BOE
- (8) Dry oxidation of gate oxide (30 nm)
- (9) DC sputtering of ZrO₂ and post annealing at 600°C
- (10) Defining of gate region with mask III and wet etching of oxide by BOE
- (11) Aluminum sputtering with hard contact mask IV (500 nm)

3.2.2 Packaging and Measurement

A container is bonded to the gate region of ISFET using epoxy resin. Figure 3-2 shows the measurement setup and a HP4156A semiconductor parameter analyzer is used for measuring the I_{DS} - V_{GS} characteristics of the ZrO₂ gate ISFETs in the buffer solutions. All the measurements are carried out at a room temperature of 25°C using a temperature control system, and what was placed in a dark box. After the buffer solution is injected into the container, measurements are not carried on until the ISFETs are immersed in the buffer solution for 60 s to make sure that the devices are under a steady state.

3.3 Results and Discussion

3.3.1 I_D - V_{DS} Characteristics of ZrO₂ Gate ISFETs

As in the discussion of the previous section, the operation of ISFET is very similar to that of conventional MOSFET, except that a reference electrode and an electrolyte are used instead of a metal gate. In the I_{DS} - V_{DS} measurement, a reference electrode is placed in buffer solutions with pHs = 1, 3, 5, 7, 9, 11, and 13, and I_{DS} - V_{DS}

curves are obtained by applying a series of step voltages at the reference electrode. Figure 3-3 shows the I_{DS} - V_{DS} curves of the ZrO_2 gate ISFETs. The devices exhibit I_{DS} - V_{DS} curves similar to those of conventional MOSFET, and the nonsaturation region is about 0.5 to 3 V at pH = 7.

3.3.2 pH Sensitivity of ZrO_2 Gate ISFET

The pH sensitivity of the ZrO_2 gate ISFET in buffer solutions with pHs = 1, 3, 5, 7, 9, 11 and 13 at room temperature is obtained using a HP4156A semiconductor parameter analyzer. Figure 3-4 shows that the I_{DS} - V_{GS} curves are shifted parallel with the pH concentration of the buffer solutions, and in the nonsaturation region with $V_{DS} = 2$ V. The I_{DS} - V_{GS} curves represent the threshold voltage shift towards positive values with increasing pH values. After 20 times measurements, a median linear pH response of 57.5 mV/pH is obtained by calculating the shifts in the V_{GS} of the ISFET using a constant drain current at 527 μ A for different pH values. Figure 3-5 shows the V_{GS} and pH values for obtaining a pH response of 57.5 mV/pH from the slope of the linear-fitted line. A 99.74% root-mean-square (R^2) value can be obtained, which represents the perfect response of the ZrO_2 gate ISFET.

3.3.3 Ratio of Width to Length in Channel Affecting ZrO_2 Gate ISFETs

To understand if the ratio of width to length in the channel affects the pH response, we measure three devices with different sizes. Figure 3-6 shows the sensitivities of the three devices that have different ratios of width over length. It seems that the sensitivity of the ISFETs is not affected by their different sizes.

3.3.4 Drift of ZrO_2 Gate ISFET

To make sure that the device is under a stable state, the ISFET must be immersed in the buffer solution for 5 h before drift measurement. The drift of the ZrO_2 gate ISFET is also calculated by I_{DS} - V_{GS} measurement for 7 h. Figure 3-7 shows a drift of 5.82 mV during the 7 h measurement in which a drift of 0.831 mV/h is

obtained. Compared with the sensitivity of the ZrO_2 gate ISFET, we can neglect the drift effect because of the small drift velocity. Figure 3-8 shows a long-term drift of the ZrO_2 membrane ISFET at 0.425 mV/h after 200 h operation. Most of the drift is observed during the first 10 h, and the result shows that the ZrO_2 film has a very stable quality.

3.3.5 pH Sensitivity of ZrO_2 Membrane ISFET in 1 M NaCl Solution

To make sure that the ZrO_2 membrane ISFET can be used in a mixed solution, we measure the pH sensitivity in 1 M NaCl buffer solution. Figure 3-9 shows the pH sensitivity of ZrO_2 membrane devices in 1 M NaCl solution. The pH sensitivities slightly decreased; however, the device has a perfect linear response of 52.5 mV/pH. The slight decrease in sensitivity may have resulted from the Na^+ ions reacting with the sensing film.



3.4 Conclusions

In this study, the ZrO_2 gate ISFET is proposed as a pH-sensitive membrane. The sensing properties of the device such as sensitivity and drift are obtained by $I_{\text{DS}}-V_{\text{GS}}$ measurement in a series of buffer solutions. A pH response of about 57.5 mV/pH and a drift of 0.831 mV/h were obtained. Different sensitivities of various ratios of width to length in the channel were not observed. Thus, the ZrO_2 gate ISFET can be used in the pH range of 1 to 13 with a perfect linear-fitted line that will enable the application of ISFETs to many fields.

3.5 References

- [1] P. Bergveld, "Development of an ion sensitive solid-state device for neurophysiological measurements," *IEEE Trans. Biomed. Eng.* vol. 17, pp. 70–71, 1970.
- [2] S. D. Moss, C. C. Johnson, and J. Janata, "Hydrogen calcium and potassium ion sensitive FET transducers," A preliminary report, *IEEE Trans. Biomed. Eng.* vol. 25 pp. 49–54, 1978.
- [3] H. K. Liao, J. C. Chou, W. Y. Chung, T. P., and S. K. Hsiung, "Study on the interface trap density of the $\text{Si}_3\text{N}_4/\text{SiO}_2$ gate ISFET," *Proceedings of the Third East Asian Conference on Chemical Sensors*, Seoul, South Korea, pp. 394–400, November 1997.
- [4] L. T. Yin, J. C. Chou, W. Y. Chung, T. P., and S. K. Hsiung, "Study of indium tin oxide thin film for separative extended gate ISFET," *Mater. Chem. Phys.* vol.70 pp. 12-16, 2001.
- [5] P. Gimmel, B. Gompf, D. Schmeiosser, H. D. Weimhofer, W. Gopel, and M. Klein, " Ta_2O_5 gates of pH sensitive device comparative spectroscopic and electrical studies," *Sensors and Actuators B* vol. 17 pp. 195–202, 1989.
- [6] J. C. Chou and J. L. Chiang, "Study on the amorphous tungsten trioxide ion-sensitive field effect transistor," *Sensors and Actuators B* vol. 66 pp. 106-108, 1998.
- [7] T. matsuo and M. Esashi, "Methods of ISFET fabrication" *Sens and Actuators* vol. 1 pp. 77-96, 1981.
- [8] J. C. Chou and J. L. Chiang, "Ion sensitive field effect transistor with amorphous tungsten trioxide gate for pH sensing" *Sens and Actuators B* vol. 62 pp. 81-87 2000.
- [9] K. M. Chang, K. Y. Chao, T. W. Chou, and C. T. Chang, "Characteristics of

Zirconium Oxide Gate Ion-sensitive Field-Effect Transistors” Japanese Journal of Applied Physics vol. 46 No. 7A pp. 4334-4338, 2007.



Table 3- I . Growth conditions for film deposition using sputtering system.

Parameter	Conditions
Deposition rate (nm/min)	0.15
Deposition pressure (Torr)	20×10^{-3}
Background pressure (Torr)	3×10^{-6}
Ar/O₂ ratio (cm³/min)	24/8
Substrate temperature (°C)	150



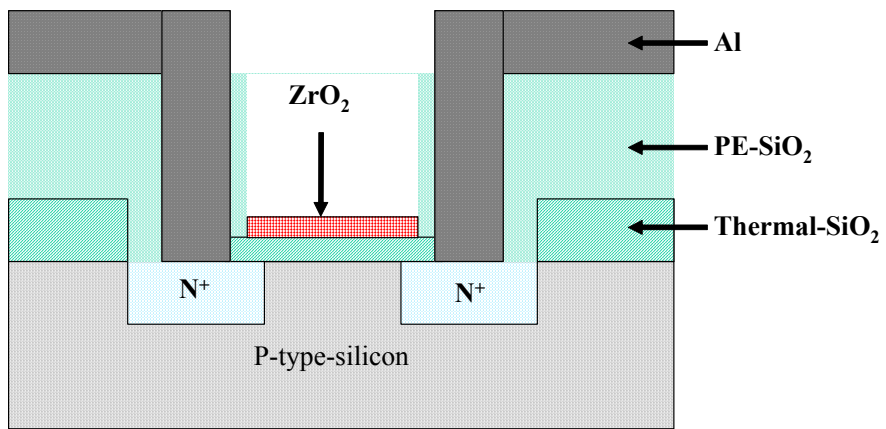


Figure 3-1 Schematic diagram of ZrO₂ gate ISFET fabricated by the MOSFET technique.



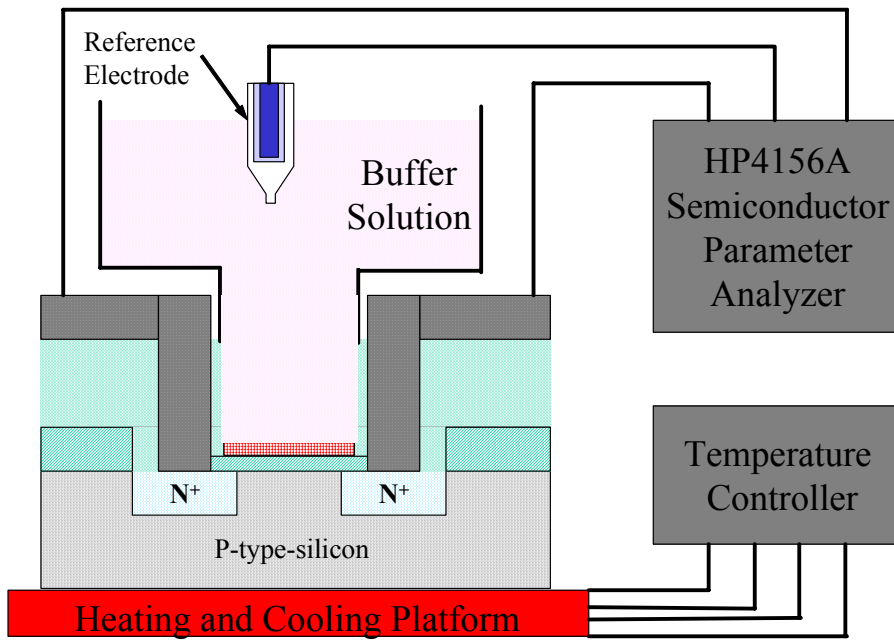
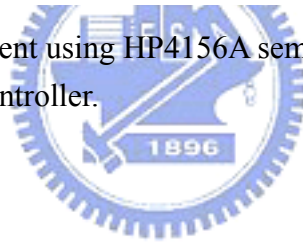


Figure 3-2 Setup of measurement using HP4156A semiconductor parameter analyzer and temperature controller.



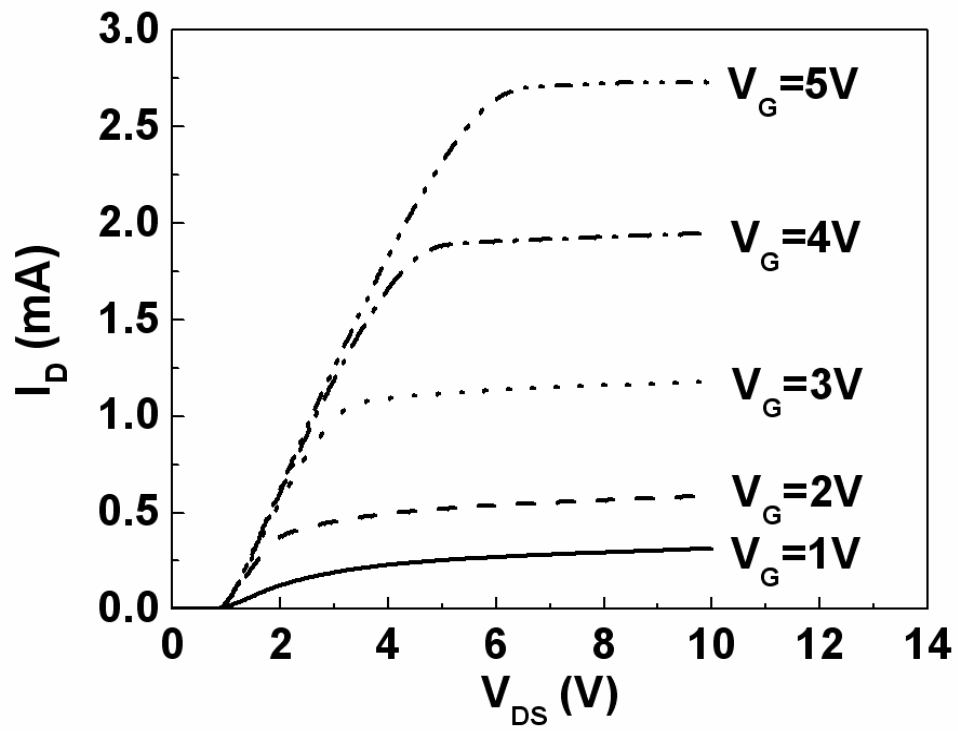


Figure 3-3 I_{DS} - V_{DS} curves of ZrO_2 gate ISFETs.



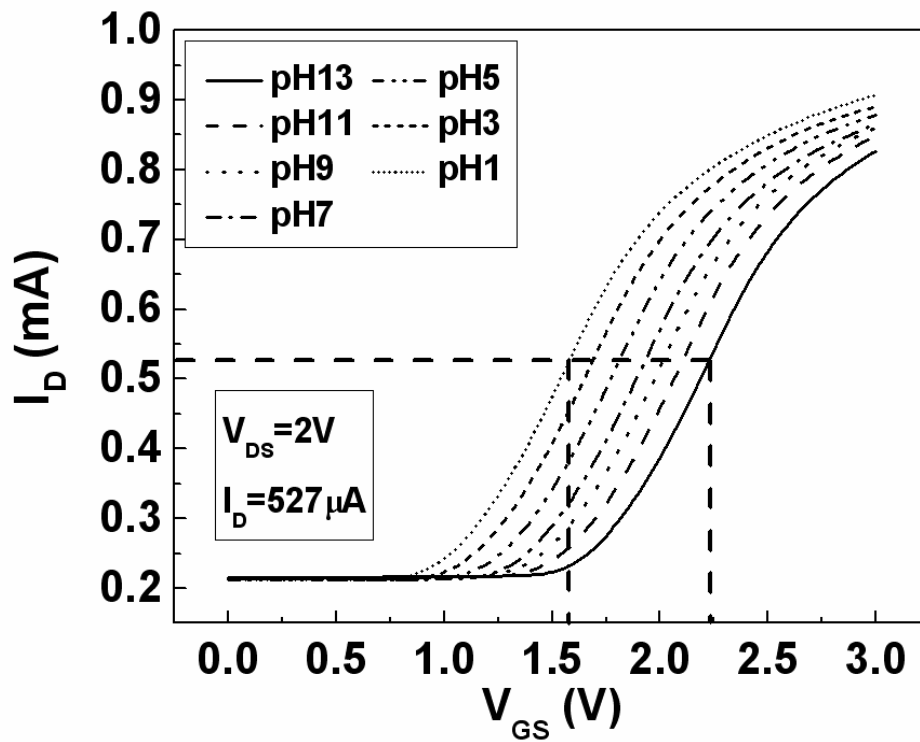


Figure 3-4 I_{DS} - V_{GS} curves that are shifted parallel with pH concentration of buffer solutions, and in nonsaturation region with $V_{DS} = 2 V$.

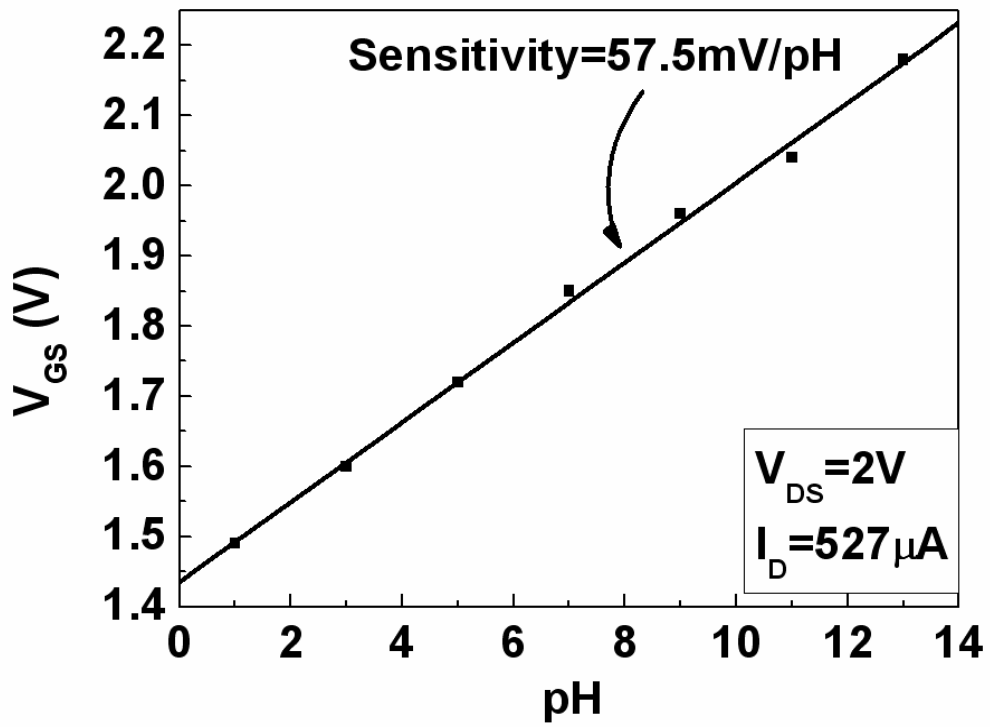


Figure 3-5 V_{GS} and pH values for obtaining pH response of 57.5 mV/pH from slope of linear-fitted line.



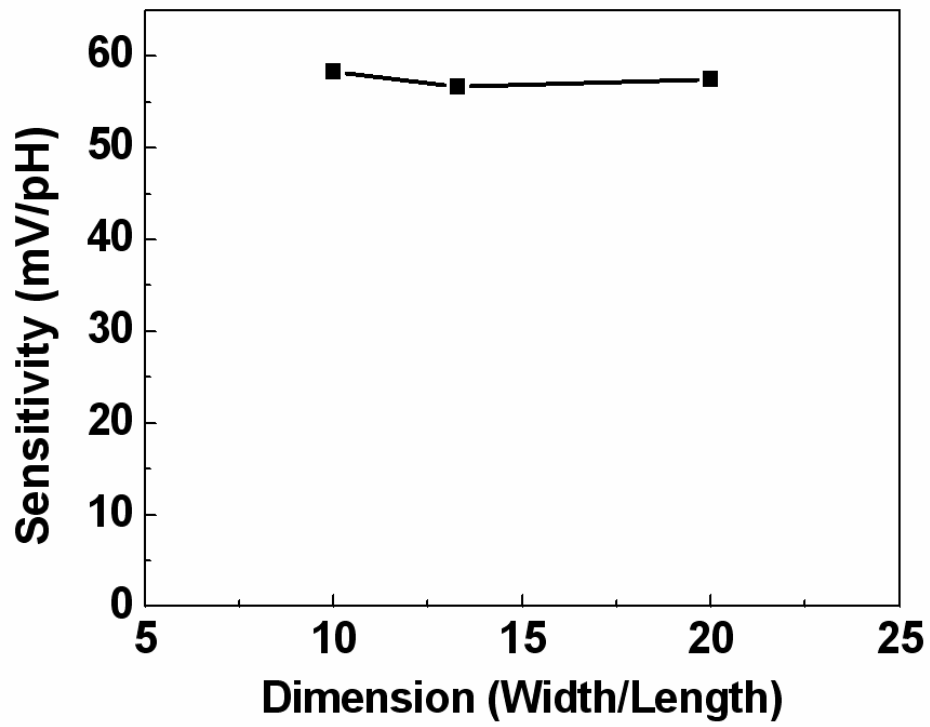


Figure 3-6 Sensitivities of three devices having different ratios of width to length.



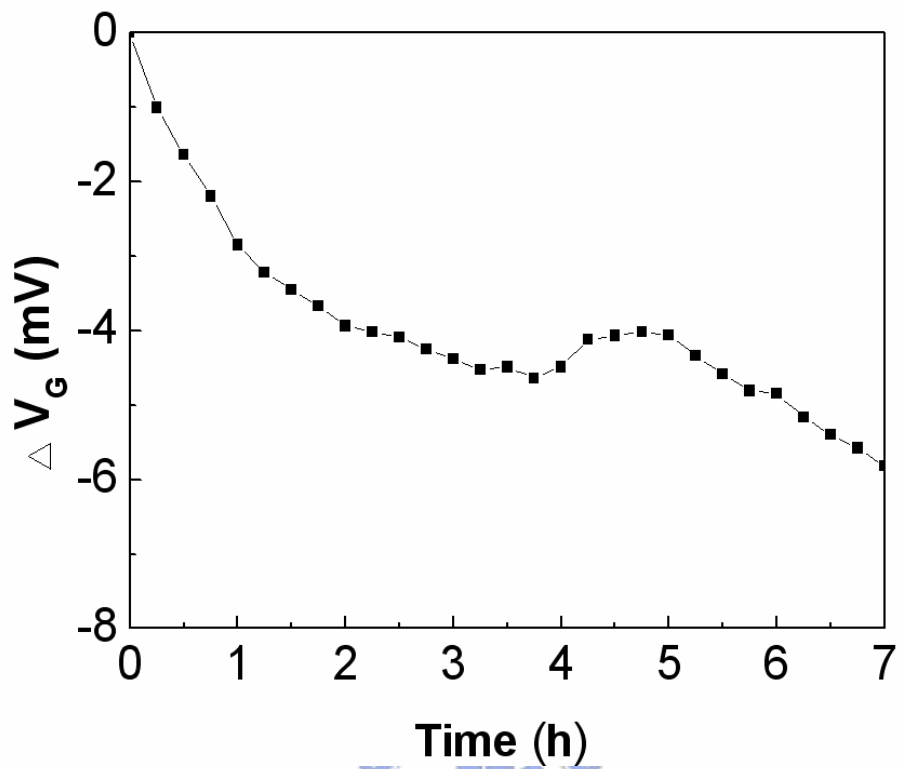


Figure 3-7 Drift of 5.82 mV during 7 h measurement in which a drift of 0.831 mV/h is obtained.



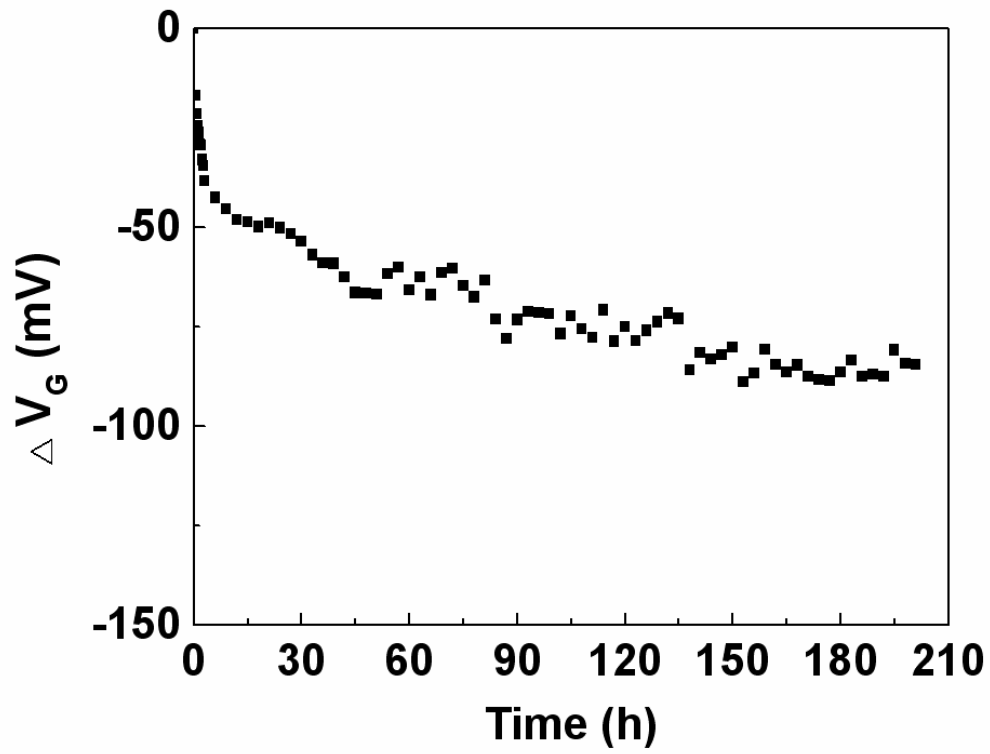
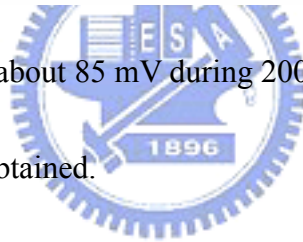


Figure 3-8 Long-term drift of about 85 mV during 200 h measurement in which a drift of 0.425 mV/h is obtained.



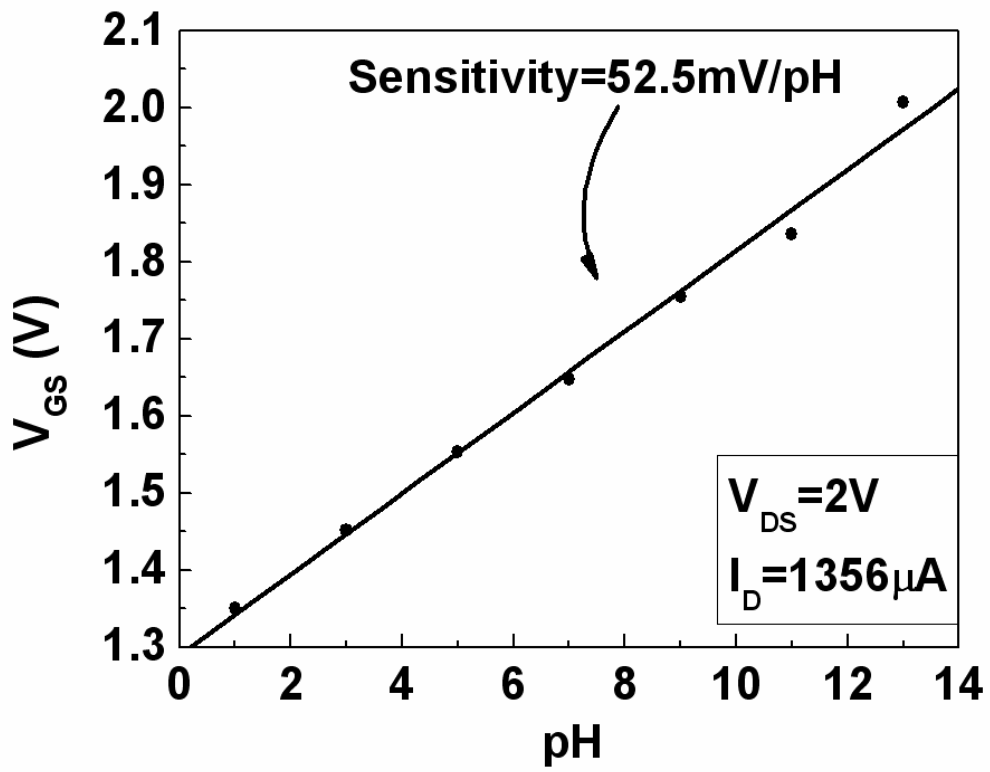


Figure 3-9 V_{GS} and pH values in 1M NaCl solution for obtaining pH response of 52.5 mV/pH from slope of linear-fitted line.



Chapter 4

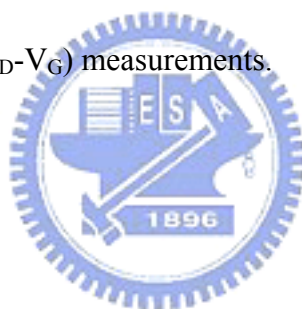
Drift Characteristics with Sensing Oxide Thickness Modulation by Co-fabricating ISFET and REFET

4.1 Backgrounds and Motivation

Because so many chemical and biological processes are dependent on pH, it is one of the most common measurements in the laboratories. In the past, the glass electrode was usually used to detect pH until a brainchild technique based on MOSFET called ISFET that had demonstrated by Bergveld in 1970 [1]. The ISFET is a special type of the MOSFET without a metal gate, by which, the gate is directly exposed to the buffer solution. When a change of the surface potential between the gate insulator and electrolyte, the electric field at the insulator semiconductor interface will be changed and the channel conductance that influences the drain current will be modulated, too. Since the channel conductance and drain current can be modulated, we may measure the changes by applying a fixed source to drain voltage or constant source to drain voltage current and different output gate voltages. By these ways, we can plot a standard linear line between gate voltages and various pH values, and the standard linear line can be taken to measure unknown acid or alkaline solution. Comparing to the conventional method, the ISFET device owns some advantages that are small size, short response time, cheap and CMOS compatible processes. The development of ISFET has been over 35 years, and the first sensitive membrane is silicon dioxide (SiO_2) which appeared instable sensitivity and large drift. Subsequently, Al_2O_3 , Ta_2O_3 , SnO_2 , TiN , $\alpha\text{-WO}_3$, ZrO_2 , and ITO were used as pH-sensitive membranes for the higher pH response and much stable drift voltage [2~9]. Table 2-I shows the sensitivities and test range of the different sensing

membranes. We can easily find that the sensitivity of SiO_2 is not the largest one and owns a large drift voltage. But in the view of CMOS compatible and bio-compatible, the SiO_2 is the most famous one. The most disadvantage of SiO_2 gate ISFET is its unstable effect that is introduced by hydration. In order to understand the relation between thickness and drift, we overcome the difficulty in measuring the unstable effect of SiO_2 gate ISFET by using the Ta_2O_5 gate REFET.

In this study, the SiO_2 membrane was used as a pH sensitive layer for ISFET. Ta_2O_5 was prepared by dc sputtering process as a pH-sensitive membrane for REFET that could estimate the effect of temperature and processing difference. The electrical characteristics and pH responses of the ISFET and REFET are studied by the standard MOSFET measurement with HP 4156A. The drift voltages are also calculated by the drain current to gate voltage (I_D - V_G) measurements.



4.2 Experimental

4.2.1 Device Fabrication

Figure 4-1 shows the schematic diagram of the SiO_2 gate ISFET which is fabricated by the MOSFET technique. A 30nm thickness sensitive layer of SiO_2 membrane was deposited onto the SiO_2 gate ISFET by PECVD. And a 30 nm thickness sensitive layer of Ta_2O_5 membrane was also sputtering onto the SiO_2 gate ISFET by sputtering system as a REFET. The SiO_2 membrane is defined by photo resist and etched by BOE. The ISFETs were fabricated on the p-type silicon wafer with (100) orientation, and the manufacture processes were listed as follows:

- (1) RCA cleaning of 4-inch, p-type silicon wafer
- (2) Wet oxidation of silicon dioxide (600 nm, Figure 4-1(a))
- (3) Defining of S/D areas with mask I and wet-etching of silicon dioxide by BOE

- (4) Thermal growth of silicon dioxide as screen oxide (30 nm, Figure 4-1 (b))
- (5) Phosphorus ion implantation and post annealing at 950°C (Figure 4-1 (c))
- (6) PECVD silicon dioxide for passivation layer (Figure 4-1 (d))
- (7) Defining of contact hole and gate region with mask II and wet-etching of silicon dioxide by BOE
- (8) Dry oxidation of gate oxide (30 nm)
- (9) PECVD silicon dioxide for sensitive layer (30 nm, Figure 4-1 (e))
- (10) Defining of gate region with mask III and wet-etching of oxide by BOE
- (11) DC sputtering a 30 nm thickness of Ta₂O₅ film with hard contact mask IV
- (12) Aluminum sputtering with hard contact mask V (600 nm, Figure 4-1 (f))

4.2.2 Packaging and Measurement

A container is bonded on the gate region of the ISFET/REFET by epoxy resin. Figure 4-2 shows the set up of measurement and the HP4156A Semiconductor Parameter Analyzer is used to measure the I_{DS} - V_{GS} characteristics of the ZrO₂ gate ISFET/REFET devices in the buffer solutions. All the measurement processes are carried out at the room temperature of 25 °C by a temperature control system, and placed in the dark box. After the buffer solution is injected into the container, we will not measure until the ISFET/REFET is immersed in the buffer solution for 60 seconds to make sure that the devices are under steady situation.

4.3 Results and Discussion

4.3.1 pH Sensitivities of the ISFET/REFET

The pH sensitivities of the ISFET and REFET in pH = 1, 3, 5, 7, 9, 11 and 13 buffer solutions at room temperature are obtained by a HP4156A Semiconductor Parameter Analyzer. Figure 4-3 shows that the I_{DS} - V_{GS} curves are shifted in parallel with the pH concentration of the buffer solutions, and in the non-saturation region

with $V_{DS} = 2$ V. The I_{DS} - V_{GS} curves represent the threshold voltage shift towards positive values with increasing pH values. After several times of measurements, a median linear pH response of 31.15 mV/pH and 55.66 mV/pH are obtained by calculating the shifts in the V_{GS} of the ISFET and REFET, respectively, by a constant drain current measurement for different pH values. Figure 4-4 shows the V_{GS} to pH values that can obtain the pH response of 31.15 mV/pH and 55.66 mV/pH by the slope of the linear fitted lines.

4.3.2 Drift of the SiO₂ Gate ISFET

The drifts of the ISFET and REFET are also calculated by I_{DS} - V_{GS} measurements for 7 hours. Figure 4-5 shows the drift during 7 hours measurement time that can be obtained a drift of 37 to 81 mV in ISFET and 8mV in REFET at the slow response region. The drift is saturation after 6 hours that implies the hydration will be stable too. In order to estimate the unwanted effect (e.g. temperature, light, process), a delta drift is defined as the differential drift of ISFET and REFET. The first hours always defined as surface reaction (fast response region) which shows a high value of drift, so we determined the last six hours as the effective times of hydration (slow response region). Figure 4-6 shows the delta drift that increases with increasing the thickness of SiO₂ film, and the curve is saturation at about 50 nm. According to the equation 43 in chapter 2, the thickness of hydration layer is about 50 nm.

4.4 Conclusion

The much stable sensing properties of sensitivity and drift are obtained by the correction of REFET. The pH response of about 28 to 32 mV/pH can be obtained. A depth of hydration layer in SiO₂ gate ISFET is presented by modulating the oxide thickness. The predicted thickness of hydration layer is 50 nm of PECVD SiO₂ during

7 hours immersing in a buffer solution. This study not only provide a simple way to determine the thickness of hydration layer without simulating, but also make the measurement of much stable drift in SiO₂ gate ISFET possible.



4.5 References

- [1] P. Bergveld, "Development of an ion sensitive solid-state device for neurophysiological measurements," IEEE Trans. Biomed. Eng. vol. 17, pp. 70–71, 1970.
- [2] S. D. Moss, C. C. Johnson, and J. Janata, "Hydrogen calcium and potassium ion sensitive FET transducers," A preliminary report, IEEE Trans. Biomed. Eng. vol. 25 pp. 49–54, 1978.
- [3] H. K. Liao, J. C. Chou, W. Y. Chung, T. P., and S. K. Hsiung, "Study on the interface trap density of the $\text{Si}_3\text{N}_4/\text{SiO}_2$ gate ISFET," Proceedings of the Third East Asian Conference on Chemical Sensors, Seoul, South Korea, pp. 394–400, November 1997.
- [4] L. T. Yin, J. C. Chou, W. Y. Chung, T. P., and S. K. Hsiung, "Study of indium tin oxide thin film for separative extended gate ISFET," Mater. Chem. Phys. vol.70 pp. 12-16, 2001.
- [5] P. Gimmel, B. Gompf, D. Schmeiosser, H. D. Weimhofer, W. Gopel, and M. Klein, " Ta_2O_5 gates of pH sensitive device comparative spectroscopic and electrical studies," Sensors and Actuators B vol. 17 pp. 195–202, 1989.
- [6] J. C. Chou and J. L. Chiang, "Study on the amorphous tungsten trioxide ion-sensitive field effect transistor," Sensors and Actuators B vol. 66 pp. 106-108, 1998.
- [7] T. matsuo and M. Esashi, "Methods of ISFET fabrication" Sens and Actuators vol. 1 pp. 77-96, 1981.
- [8] J. C. Chou and J. L. Chiang, "Ion sensitive field effect transistor with amorphous tungsten trioxide gate for pH sensing" Sens and Actuators B vol. 62 pp. 81-87, 2000.
- [9] K. M. Chang, K. Y. Chao, T. W. Chou, and C. T. Chang, "Characteristics of

Zirconium Oxide Gate Ion-sensitive Field-Effect Transistors” Japanese Journal of Applied Physics Vol. 46 No. 7A pp. 4334-4338, 2007.



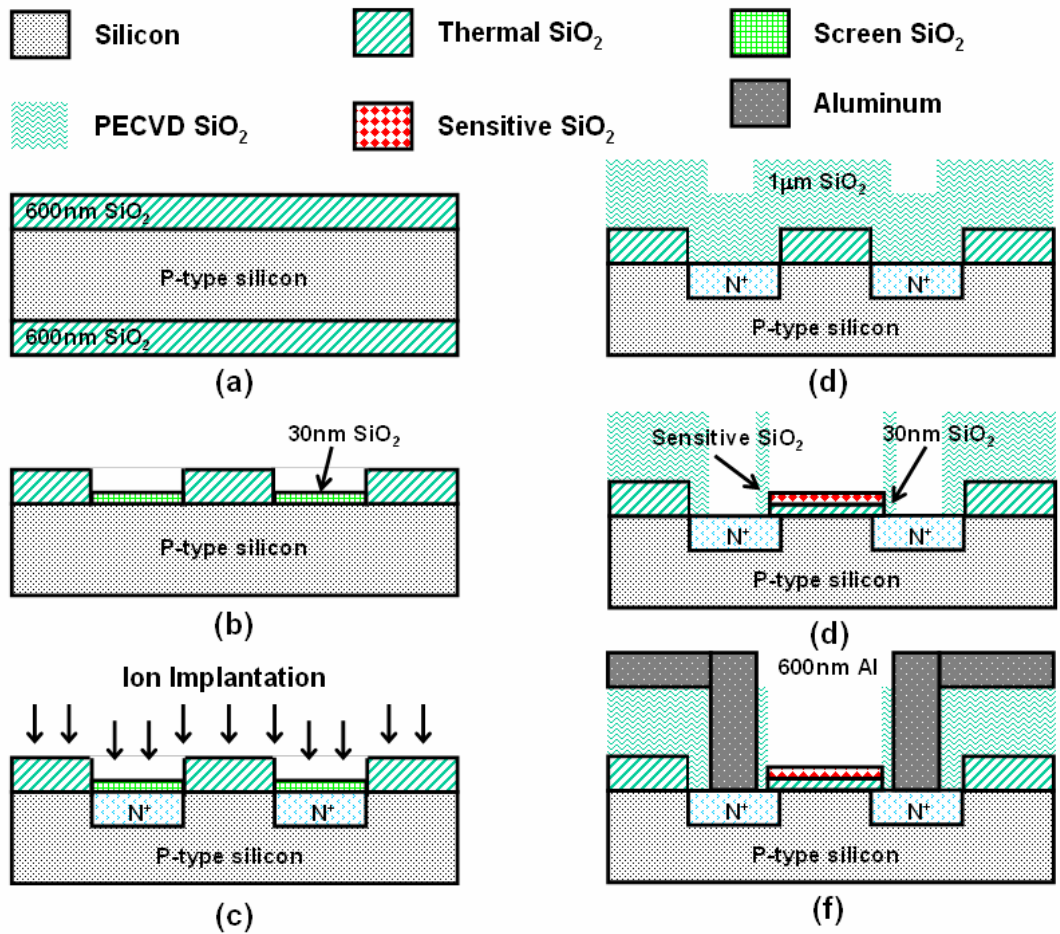


Figure 4-1 The schematic diagram of the SiO₂ gate ISFET which is fabricated by the MOSFET technique.

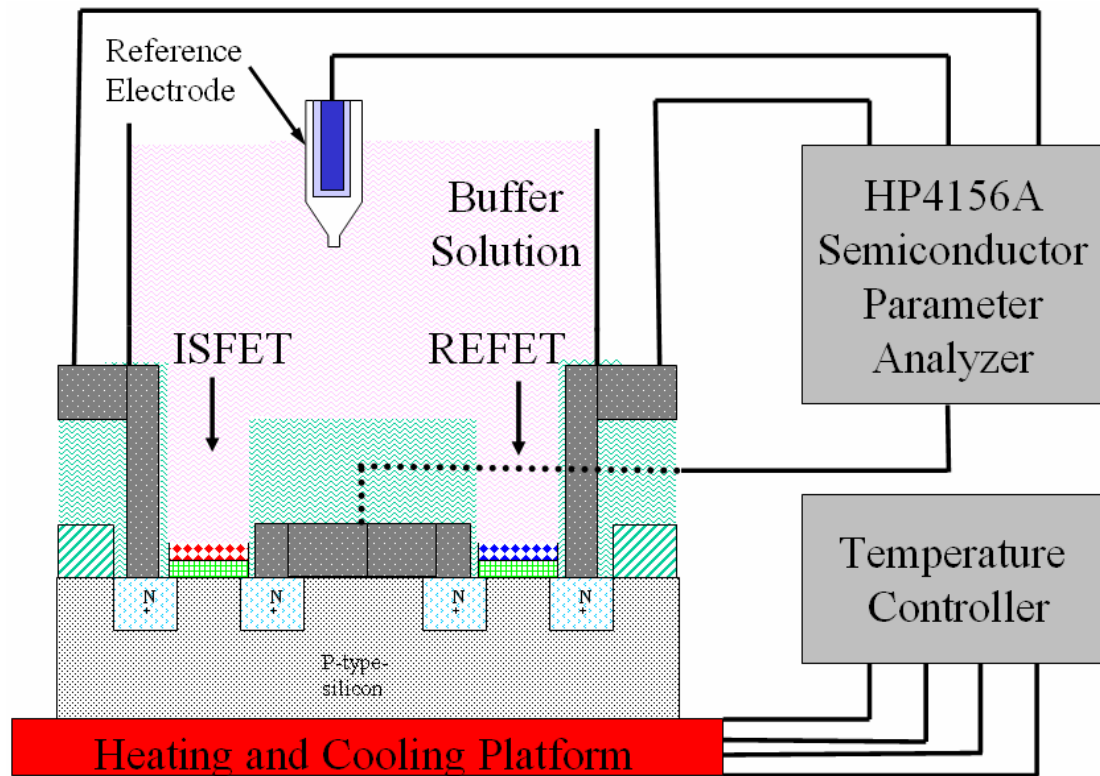


Figure 4-2 The set up of measurement with the HP4156A Semiconductor Parameter Analyzer and temperature controller.

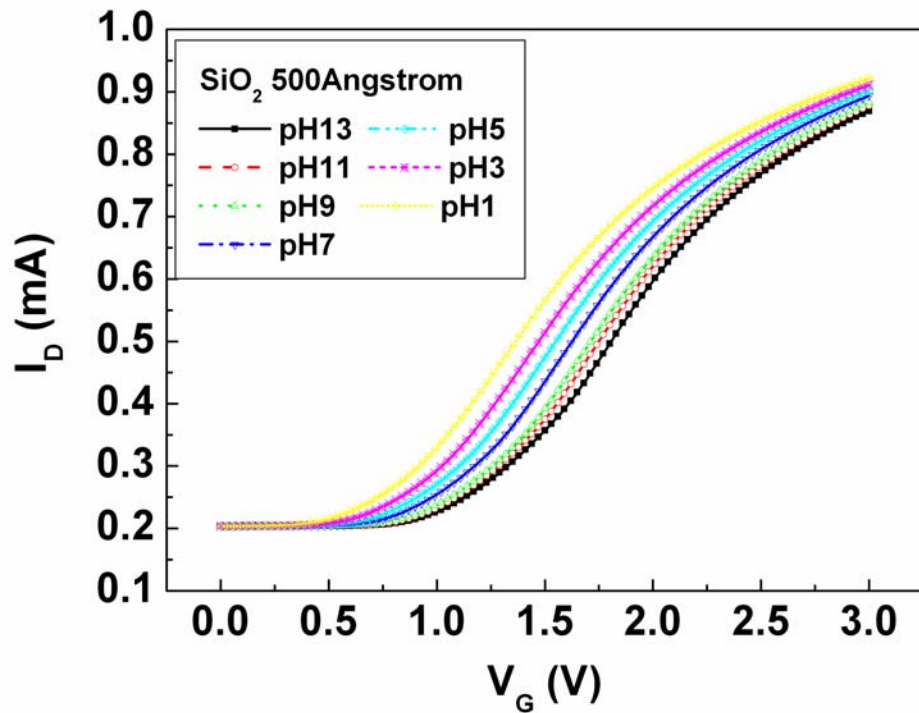


Figure 4-3 (a) The I_{DS} - V_{GS} curves of SiO_2 gate ISFET devices (50 nm).

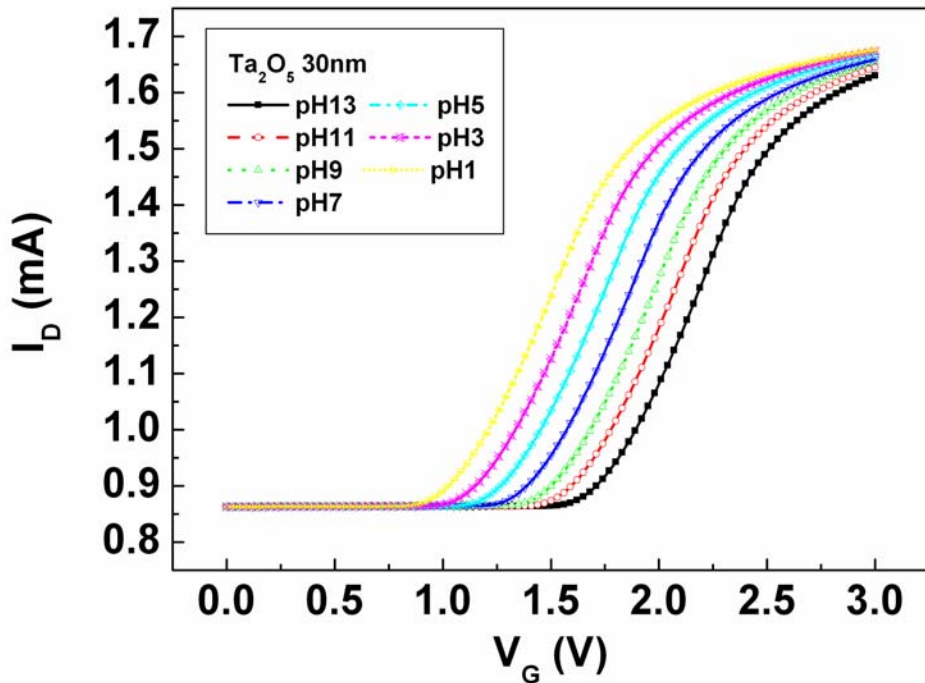


Figure 4-3 (b) The I_{DS} - V_{GS} curves of Ta_2O_5 gate ISFET devices (30 nm).

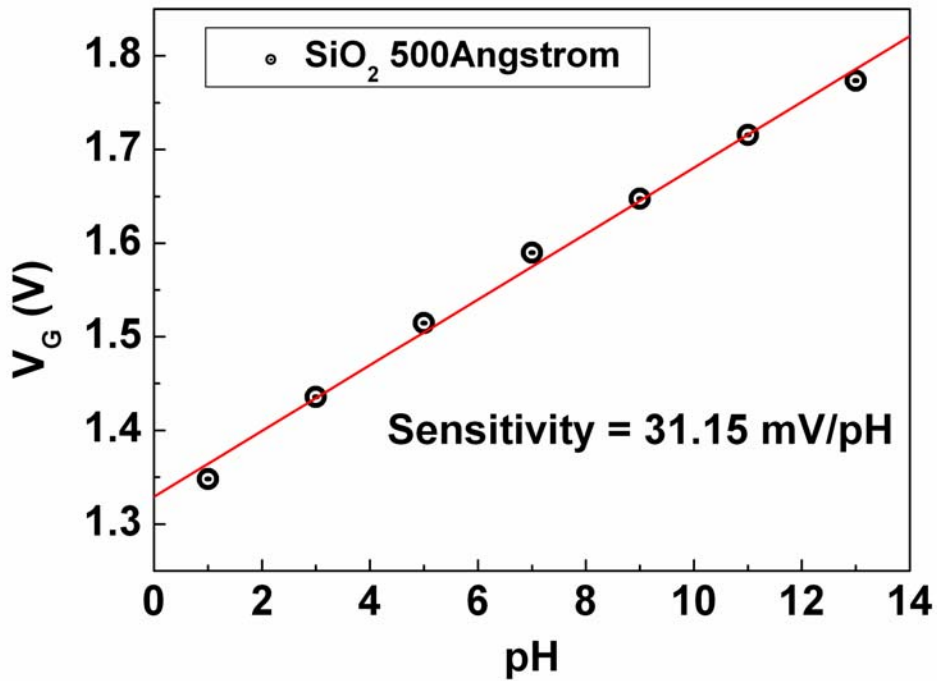


Figure 4-4 (a) Sensitivity of SiO₂ gate ISFET device (50 nm).

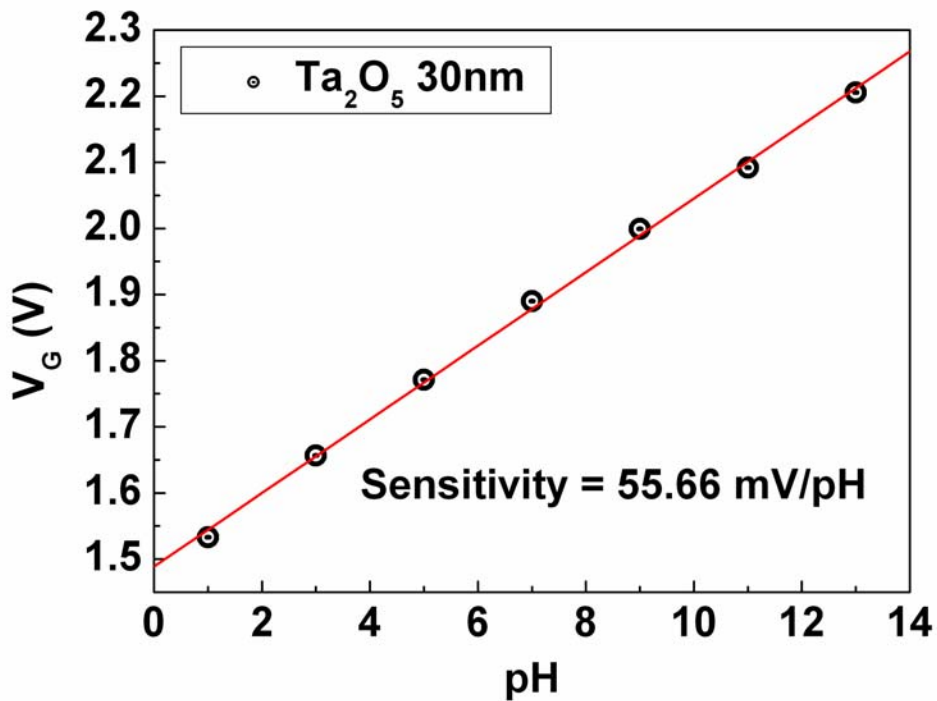
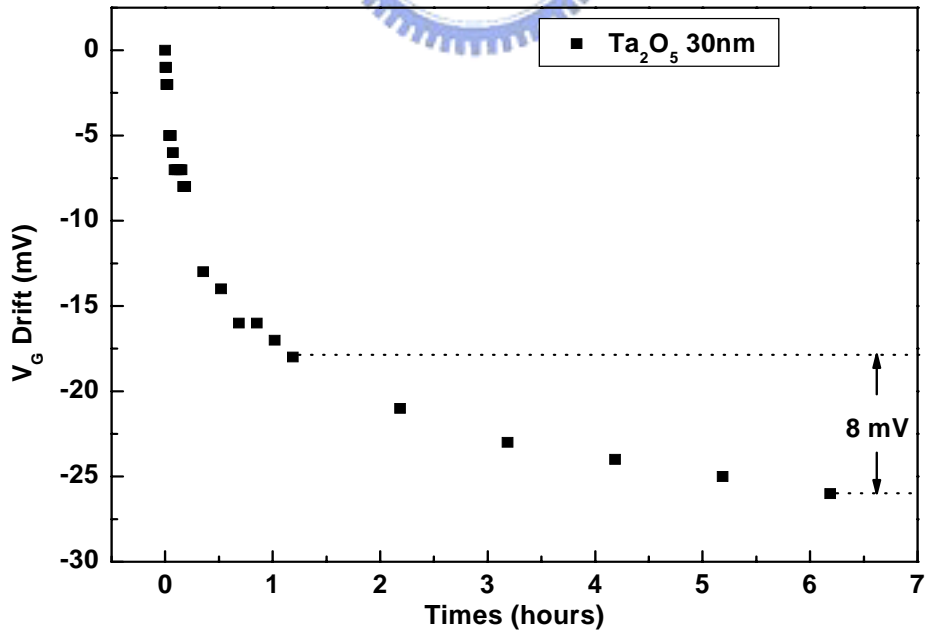
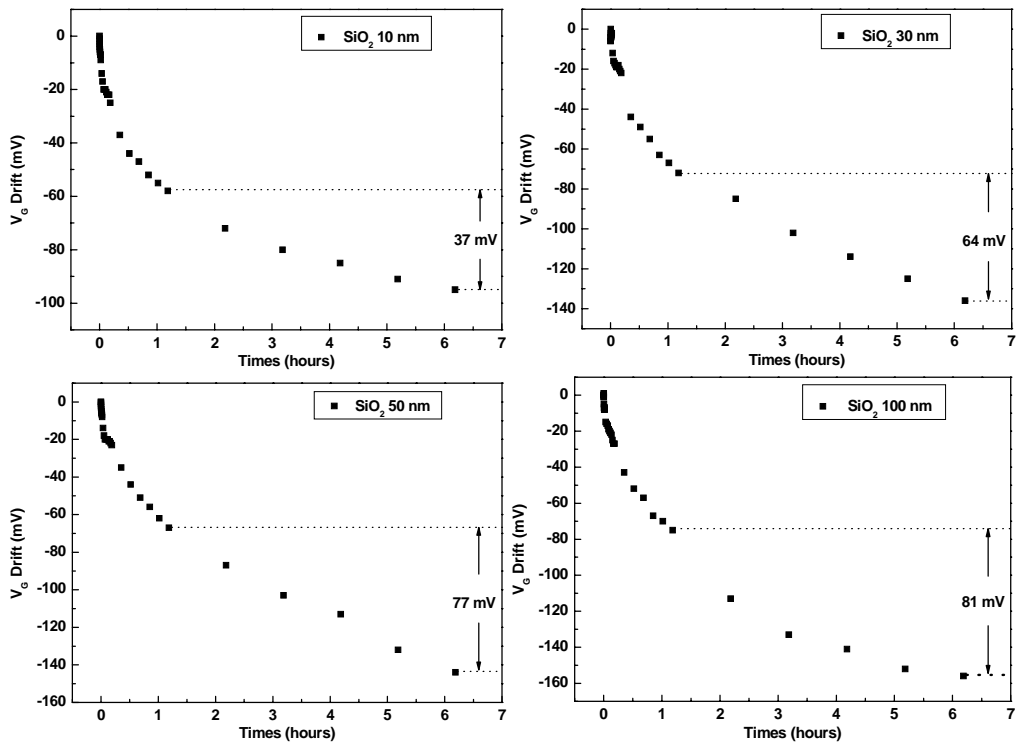


Figure 4-4 (b) Sensitivity of Ta₂O₅ gate ISFET device (30 nm).



(b)

Figure 4-5 Drifts in ISFET and REFET during 7 hours.

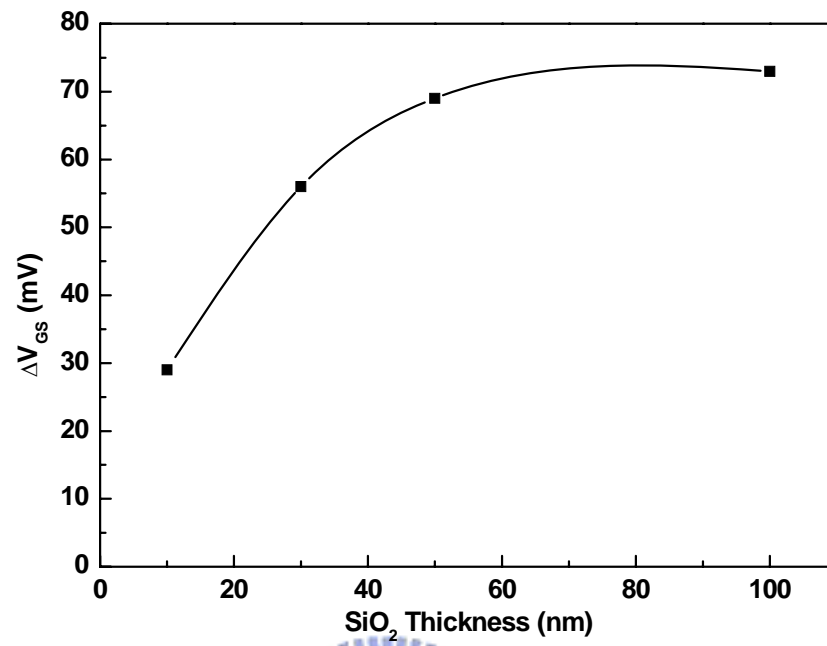


Figure 4-6 Delta drifts of SiO_2 gate ISFET devices.



CHAPTER 5

Ultra-Low Drift Voltage by Using Gate Voltage control in Oxide-Based Gate ISFET

5.1 Backgrounds and Motivation

There are a lot of chemical and biological processes dependent on pH, and thus the pH detection device is one of the most common measurements in laboratories. In the past, a glass electrode was usually used for detecting pH until a brainchild technique based on metal-oxide-semiconductor field-effect transistor (MOSFET) called ion-sensitive field-effect transistor (ISFET) that was demonstrated by Bergveld in 1970 [1]. The first sensing membrane used is silicon dioxide (SiO_2), which showed an unstable sensitivity due to a large drift. Subsequently Al_2O_3 , Ta_2O_5 , SnO_2 , TiN , α - WO_3 , ITO, and ZrO_2 [2-4] have been tried to use as the pH-sensitive membranes to achieve a higher pH response and a more stable drift voltage. Although drift voltage is much smaller than sensitivity, the drawback is continuously affecting the ISFET to commercialize. There are some proposed explanations for drift including electric field enhanced ion migration within the gate insulator [5], some electrons creating space charge inside the insulator films, and some surface effects [6]. There are also some methods to solve the drift problem, such as manufacturing with a reference field-effect transistor (REFET) or disposing a correct integrated circuit device to reduce the drift rate. However, these methods are always either having a difficult process or costing too expensive.

In this study, a simple and cheap way to solve the drift problem is presented which describes the relation of drift and gate voltage. Constant various gate voltages are biased in the sensing layer with reference electrode. It obviously shows a strong relation of gate drift and gate stress voltages. There are two sensing films of ZrO_2 and

SiO₂ to be considered in this study. A great improvement of drift voltage in these two materials as ISFETs can be achieved by using gate voltage controlling method.

From equation 39 in chapter 2, we observed that drift is directly proportional to the thickness of the hydrated layer which may contain both H⁺ and OH⁻ ions. The series combinations of the capacitances are illustrated in Figure 5-1 (a). Figure 5-1 (b) shows series combinations of capacitances after ISFETs immersing in the buffer solution. It is proposed that ions will penetrate into sensitive layer and form a hydrated layer which will distribute either positive or negative charges.

According to Bousse and Bergveld [6], there are two responses of inorganic-gate ISFETs. One is fast response which is called sensitivity and another is slow response which is called drift. The slow response of drift has several models to explain. One model based on the reactivity of the insulator in the electrical double layer in the electrolyte at the interface with the insulator [7]. Another model based on the presence of H⁺ ions in the insulating layer [8]. The last one model based on the modification of the interface of Si and SiO₂ through a pH controlled charge in the surface state density via transport of a hydrogen-bearing species [9]. All of these models point out that the drift voltages are affected by the charges either in insulator or on interface of insulator. Thus, this study considered to apply a gate-to-silicon substrate voltage to create an electrical field to erase the drift effect caused by trapping charges. Figure 5-1(c) shows the schematic diagram of the electrical force will enhance or reduce the penetration of ions into sensitive film forming a hydrated layer. Thus, if we properly control the electrical force by gate voltage, then the drift effect by charges migrating will be solved. In this study, we try to control the gate voltages during measuring drift voltage to achieve a zero drift voltage measurement.

5.2 Experimental Procedure

5.2.1 Device Fabrication

Figure 5-2 shows a fabricating process of ISFET which is a CMOS compatible technique. A 30-nm-thick sensitive layer of the SiO₂ membrane was deposited onto the SiO₂ gate ISFET by PECVD. And a 30-nm-thick sensitive layer of the ZrO₂ membrane was also sputtering onto the SiO₂ gate ISFET using DC sputtering system. The sensing membrane is defined by photoresist and etched by buffer oxide etch (BOE). The ISFETs were fabricated on the p-type silicon wafer with (100) orientation and the manufacturing processes are listed as follows:

- (1) RCA cleaning of 4-inch p-type silicon wafer
- (2) Wet oxidation of silicon dioxide (600 nm, Figure 5-2(a))
- (3) Defining of S/D area with mask I and wet-etching of silicon dioxide by BOE
- (4) Thermal growth of silicon dioxide as screen oxide (30 nm, Figure 5-2 (b))
- (5) Phosphorus ion implantation and post annealing at 950°C (Figure 5-2 (c))
- (6) PECVD of silicon dioxide for passivation layer (Figure 5-2 (d))
- (7) Defining of contact hole and gate region with mask II and wet-etching of silicon dioxide by BOE
- (8) Dry oxidation of gate oxide (30 nm)
- (9) PECVD silicon dioxide or DC sputtering ZrO₂ film for sensitive layer (30 nm, Figure 5-2 (e))
- (10) Defining of gate region with mask III and wet-etching of oxide by BOE
- (11) Aluminum sputtering with hard contact mask IV (600 nm, Figure 5-2 (f))

5.2.2 Packaging and Measurement

A container is bonded to the gate region of ISFET using epoxy resin. Figure 5-3 shows the measurement setup and a HP4156A semiconductor parameter analyzer is used for measuring characteristics of ISFETs in the buffer solutions. All the

measurements are carried out at a room temperature of 25°C using a temperature control system, and what was placed in a dark box. An Ag/AgCl reference electrode is used as a constant DC voltage reference in the measurement system. After the buffer solution is injected into the container, measurements are not carried on until the ISFETs are immersed in the buffer solution for 60 s to make sure that the devices are under a steady state

5.3 Results and Discussion

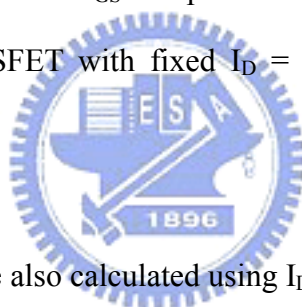
5.3.1 I_D - V_{DS} Characteristics of the ISFET Devices

As in the discussion of the previous section, the operation of ISFET is very similar to that of conventional MOSFET, except that a reference electrode and an electrolyte are used instead of a metal gate. In the I_D - V_{DS} measurement, a reference electrode is placed in buffer solutions with pHs = 1, 3, 5, 7, 9, 11 and 13, and I_{DS} - V_{DS} curves are obtained by applying a series of step voltages at the reference electrode. Figure 5-4 (a) shows the I_D - V_{DS} curves of the SiO₂ gate ISFETs. And figure 5-4 (b) shows the I_D - V_{DS} curves of the ZrO₂ gate ISFETs. There exhibits the similar I_D - V_{DS} curves as the conventional MOSFET, and the non-saturation region is about 0 to 3 V at pH = 7. The perfect characteristics of ISFETs indicate that even the metal gate has already been replaced using a buffer solution and a reference electrode, the device still owned pretty good characteristics of MOSFET. Thus, all measurements are following conventional methods of MOSFET.

5.3.2 pH Sensitivity of the ISFETs

The pH sensitivities of SiO₂ and ZrO₂ gate ISFET in buffer solutions with pHs = 1, 3, 5, 7, 9, 11 and 13 at room temperature are obtained using a HP4156A semiconductor parameter analyzer. Figure 5-5 (a) shows that the I_D - V_{GS} curves of SiO₂ gate ISFET are shifted parallel with the pH concentration of the buffer solutions,

and in the nonsaturation region with $V_{DS} = 1$ V. The I_D - V_{GS} curves represent the threshold voltage shift towards positive values with increasing pH values. Figure 5-5 (b) shows that the I_D - V_{GS} curves of ZrO_2 gate ISFET are shifted parallel with the pH concentration of the buffer solutions, and in the nonsaturation region with $V_{DS} = 2$ V. The I_D - V_{GS} curves also represent the threshold voltage shift towards positive values with increasing pH values. After several times measurements, median linear pH responses of 31.15 and 57.5 mV/pH are obtained by calculating the shifts in the V_{GS} of SiO_2 and ZrO_2 gate ISFETs using constant drain current measurements for different pH values. Figure 5-6 (a) shows the V_{GS} and pH values for obtaining pH responses of 31.15 of SiO_2 gate ISFET with fixed $I_D = 508$ μ A from the slope of the linear-fitted line. And Figure 5-6 (b) shows the V_{GS} and pH values for obtaining pH responses of 57.5 mV/pH of ZrO_2 gate ISFET with fixed $I_D = 527$ μ A from the slope of the linear-fitted line.



5.3.3 Drift of ISFET

The drift of the ISFETs are also calculated using I_D - V_{GS} measurement for 10 hours. During the 10 hours measuring time, various DC biased voltages are applying between the reference electrode and substrate. To make sure that the reference pH devices are in a stable state, the devices must be immersed in the buffer solution for one hour before drift measuring. There are two sensing films of SiO_2 and ZrO_2 to be consideration in the study. Figure 5-7 (a) shows drift of SiO_2 gate ISFET during 10 hours measurement time that can be obtained a drift of 56.12 to -27.15 mV at the slow response region. Figure 5-7 (b) shows drift of ZrO_2 gate ISFET during 10 hours measurement time that can be obtained a drift of 0.76 to -57.94 mV at the slow response region. It obviously showed a strong relation of drift voltages and gate stress voltages. The values of drift voltages always show from a positive number to a negative number. In other words, a zero value of drift can always be found using this

method. Thus, a great improvement of drift voltage in these two membranes as ISFETs can be achieved by using the gate voltage controlling method. When gate voltage is controlled as 0.5 V, drift voltage of SiO₂ gate ISFET will decrease from 56.12 to 2.94 mV in ten hours measurement. The improvement of the drift voltage reaches 94.8%. Also, when gate voltage is controlled as -1 V, drift voltage of ZrO₂ gate ISFET will decrease from -57.94 to 0.76 mV in ten hours measurement. The improvement of the drift voltage reaches 98.7%. This may result from the gate electric field affecting the ions to diffusive into the gate insulator, and the gate voltage shift will be blocked. When the properly electric field was applied between reference electrode and substrate, the drift effect would be erased. Figure 5-8 shows the relation of drift voltages and the gate stress voltages. With the different gate stress voltages, both of the two sensing films have various differential gate voltages shift named drift voltages. We can always find a gate stress voltage that makes the differential gate voltage shift close to zero deviation. In this study, the gate voltage should be controlled as 0.5 V in the SiO₂ gate ISFET and -1 V in the ZrO₂ gate ISFET.

5.4 Conclusion

An ultra-low drift voltage by using gate voltage controlling method in oxide-based gate ISFETs is realized. There are two sensitive oxide membranes of ZrO₂ and SiO₂ using in this research. We can always find a gate stress voltage that makes the differential gate voltage shift be close to zero deviation. The improvements of drift voltage reach 98.7% of ZrO₂ and 94.8% of SiO₂. It is a very great improvement of drift that will improve the ISFETs more applications. When the optimum gate voltage was applied to the ISFETs, the drift problem of ISFET would be solved in the future.

5.5 References

- [1] P. Bergveld, "Development of an ion sensitive solid-state device for neurophysiological measurements," *IEEE Trans. Biomed. Eng.* vol. 17, pp. 70–71, 1970.
- [2] T. matsuo and M. Esashi, "Method of ISFET fabrication," *Sens. Actuators*, vol. 1, pp. 77-96, 1981.
- [3] H. K. Liao, J. C. Chou, W. Y. Chung, T. P., and S. K. Hsiung, "Study on the interface trap density of the $\text{Si}_3\text{N}_4/\text{SiO}_2$ gate ISFET," *Proceedings of the Third East Asian Conference on Chemical Sensors*, Seoul, South Korea, pp. 394–400, November 1997.
- [4] L. T. Yin, J. C. Chou, W. Y. Chung, T. P., and S. K. Hsiung, "Study of indium tin oxide thin film for separative extended gate ISFET," *Mater. Chem. Phys.* vol.70 pp. 12-16, 2001.
- [5] M. Esashi and T. Matsuo, "Integrated Micro Multi. Ion Sensor Using Field Effect of Semiconductor," *IEEE Trans. Biomed. Eng.*, vol. 25, pp. 184-192, 1978.
- [6] L. Bousse and P. Bergveld, "Role of buried OH sites in the response mechanism of inorganic-gate pH-sensitive ISFETs, " *Sens. Actuators*, vol. 6, pp. 65-78, 1984.
- [7] R. G. Kelly," *Microelectronic Approaches to Solid State Ion Selective Electrodes*," *Electrochimica Acta*, vol. 22, pp.1-8, 1977.
- [8] P. Bergveld, N. F. de Rooij, and J. N. Zemel," *Physical mechanisms for chemically sensitive semiconductor devices*," *Nature*, vol. 273, pp. 438-443, 1978.
- [9] A. G. Revesz," *The mechanism of the ion-sensitive. field effect transistor*," *Thin Solid Films*, vol. 41, pp. L43-L47, 1977.

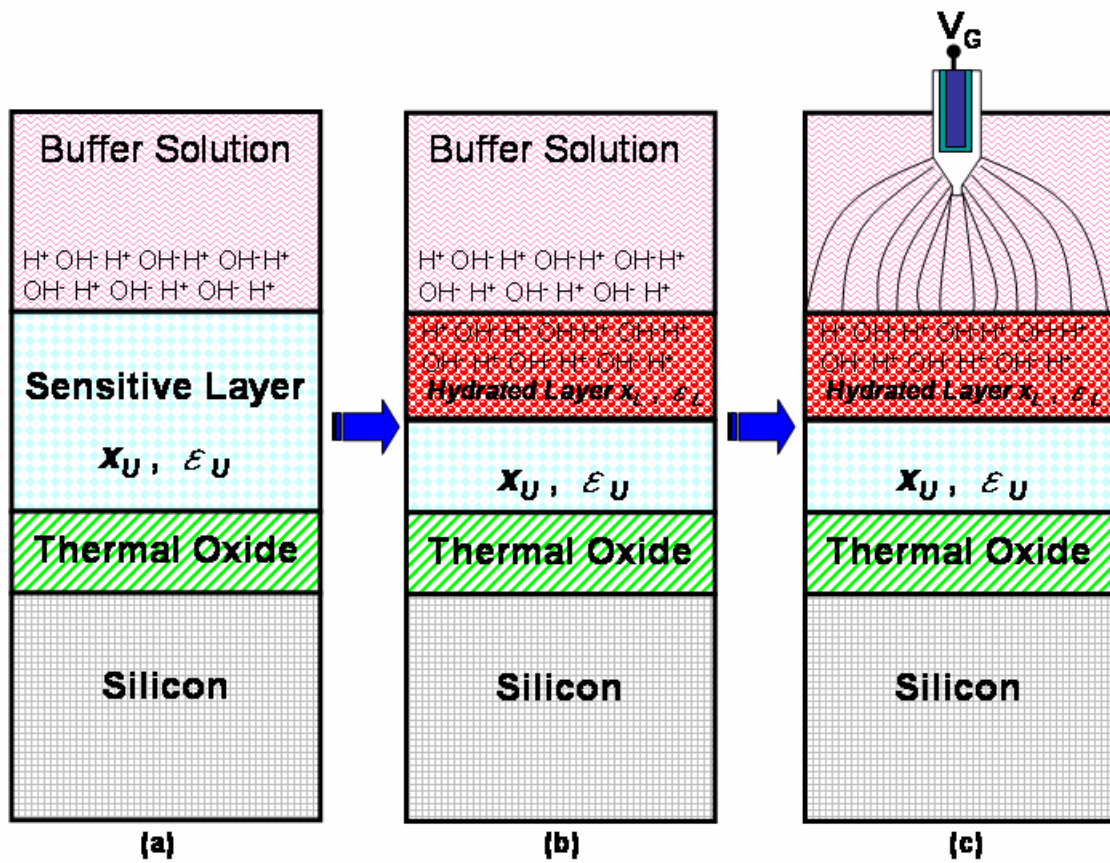


Figure 5-1. Series combinations of (a) initial, (b) hydrated without gate voltage control, and (c) hydrated with gate voltage control

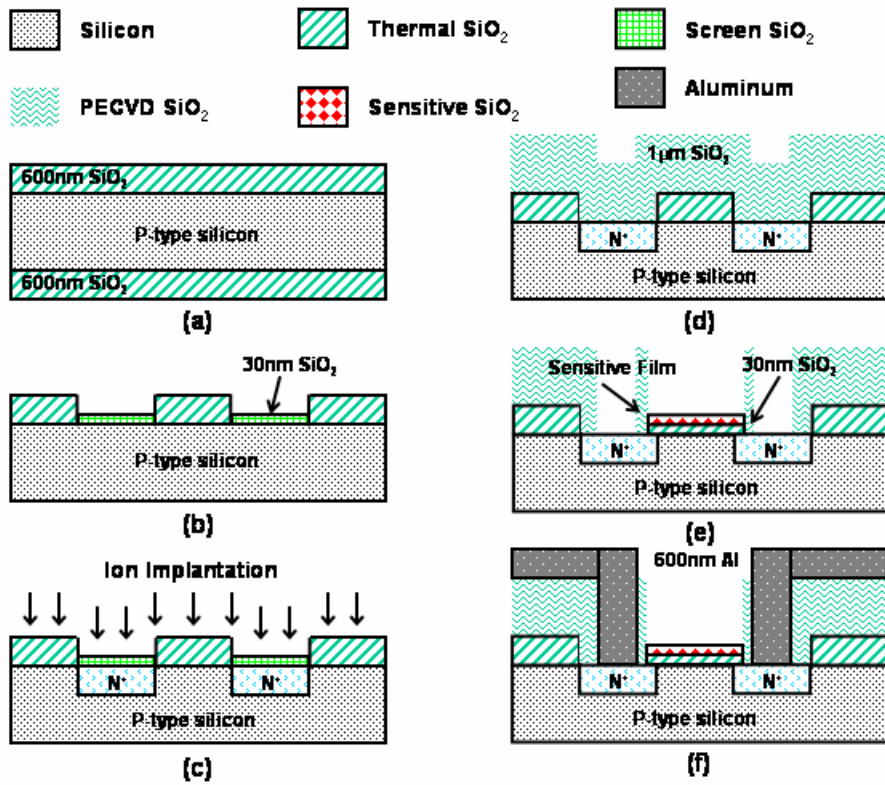


Figure 5-2. Fabricated processes of ISFET which is a CMOS compatible technique.



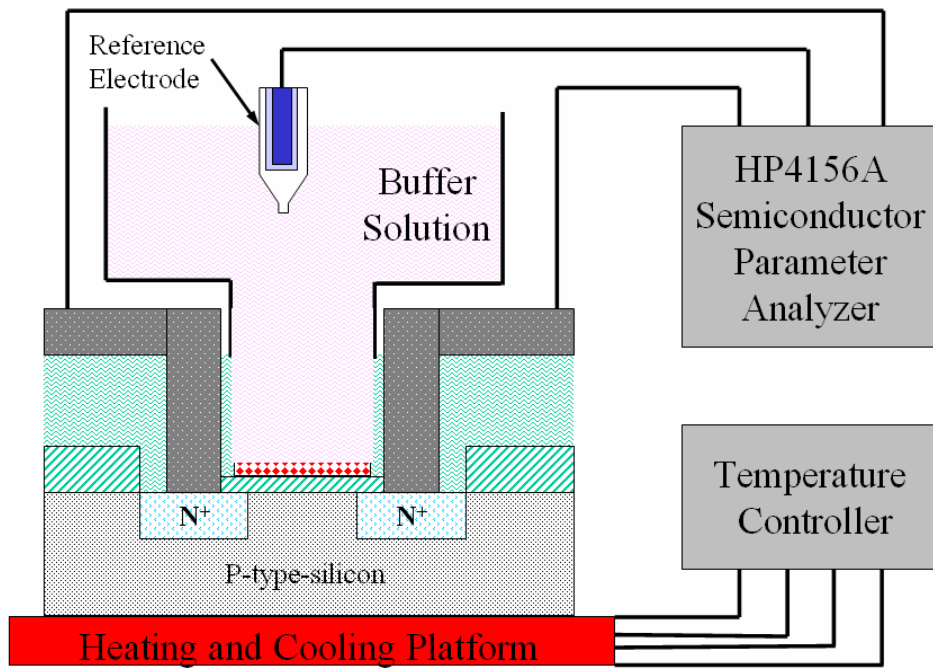


Figure 5-3. Setup of measurement Using HP4156A semiconductor parameter analyzer and temperature controller.

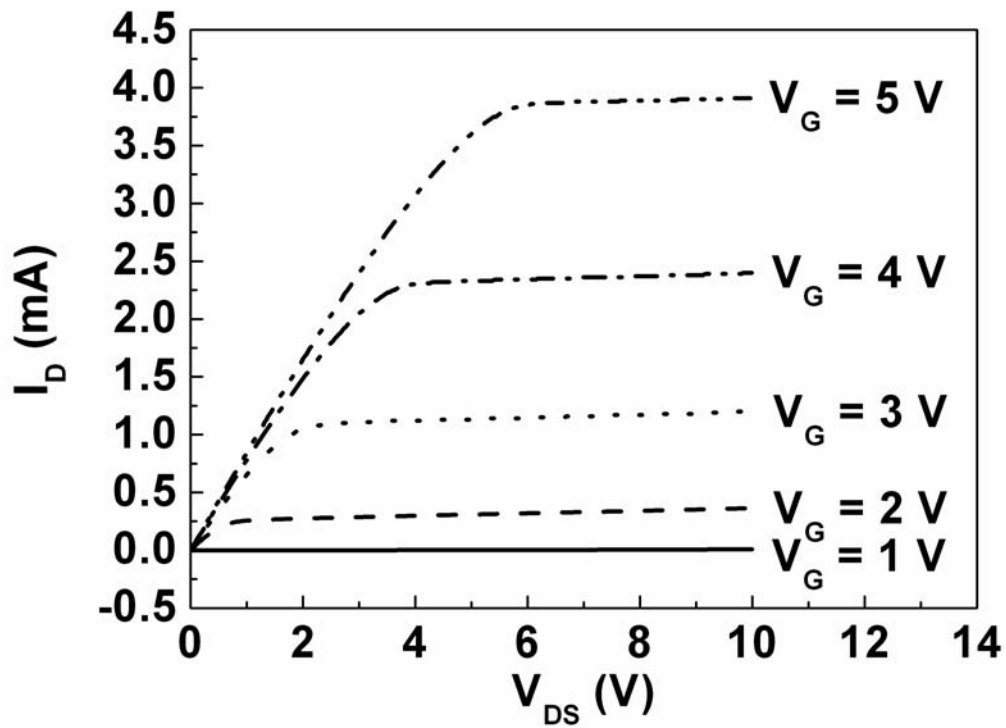


Figure 5-4 (a). I_D - V_{DS} curves of SiO_2 gate ISFETs.

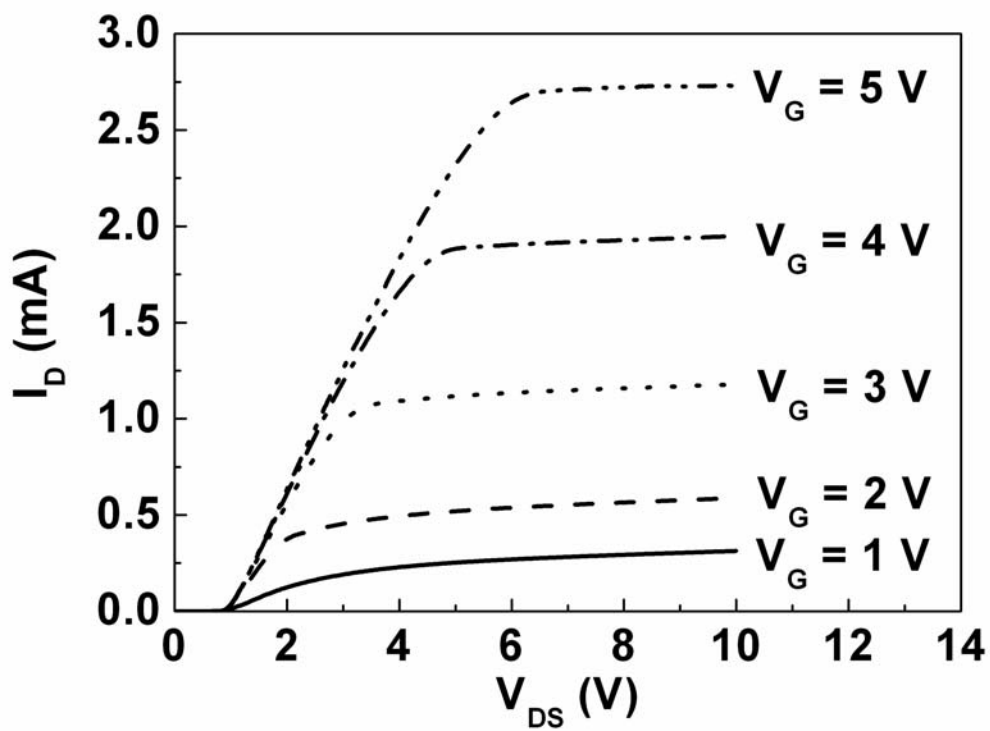


Figure 5-4 (b). I_D - V_{DS} curves of ZrO_2 gate ISFETs.

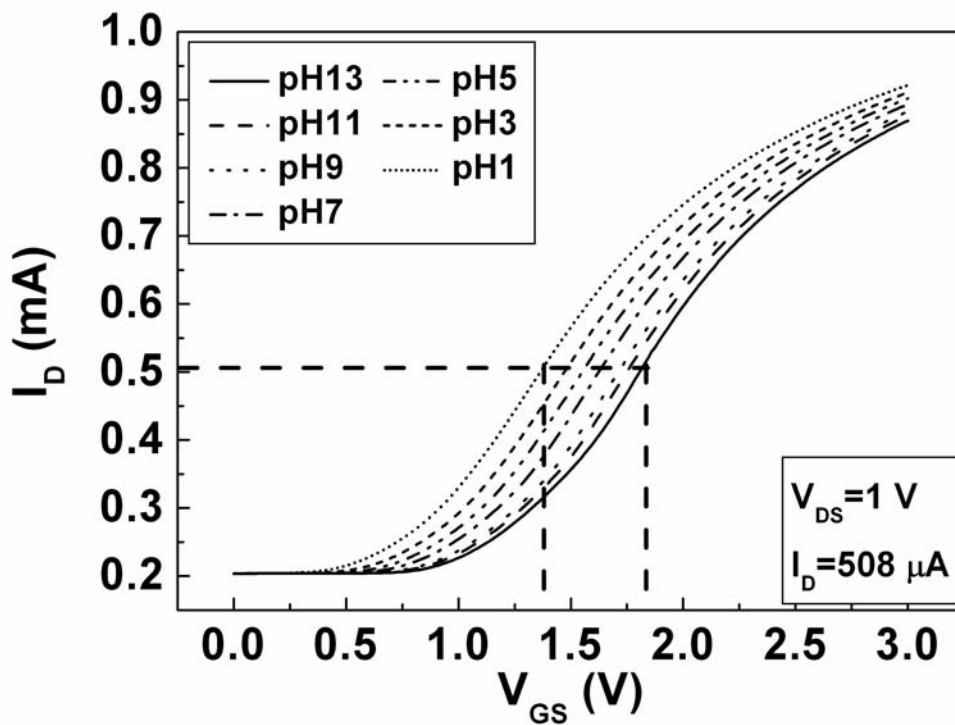


Figure 5-5 (a). I_D - V_{GS} curves of SiO_2 gate ISFETs.

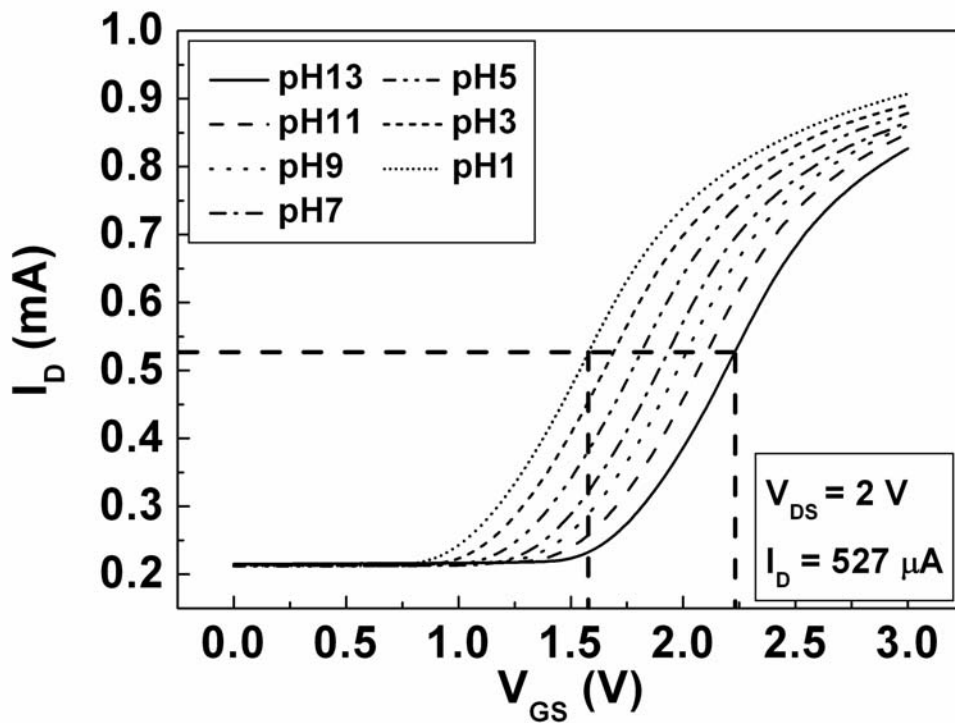


Figure 5-5 (b). I_D - V_{GS} curves of ZrO_2 gate ISFETs.

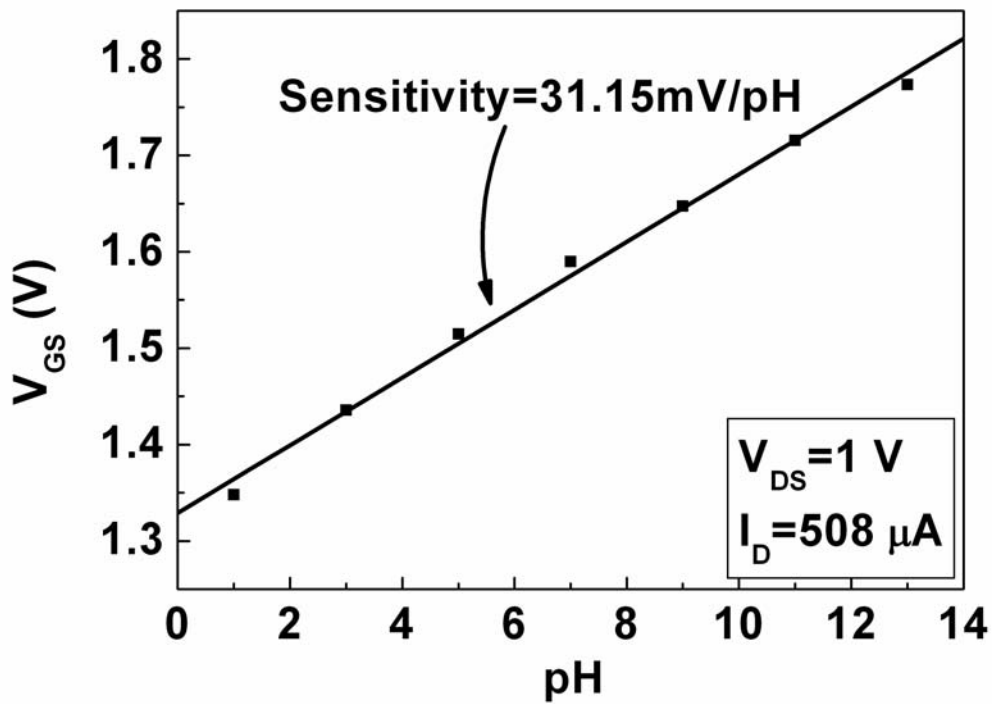


Figure 5-6 (a). Sensitivity of SiO₂ gate ISFETs.

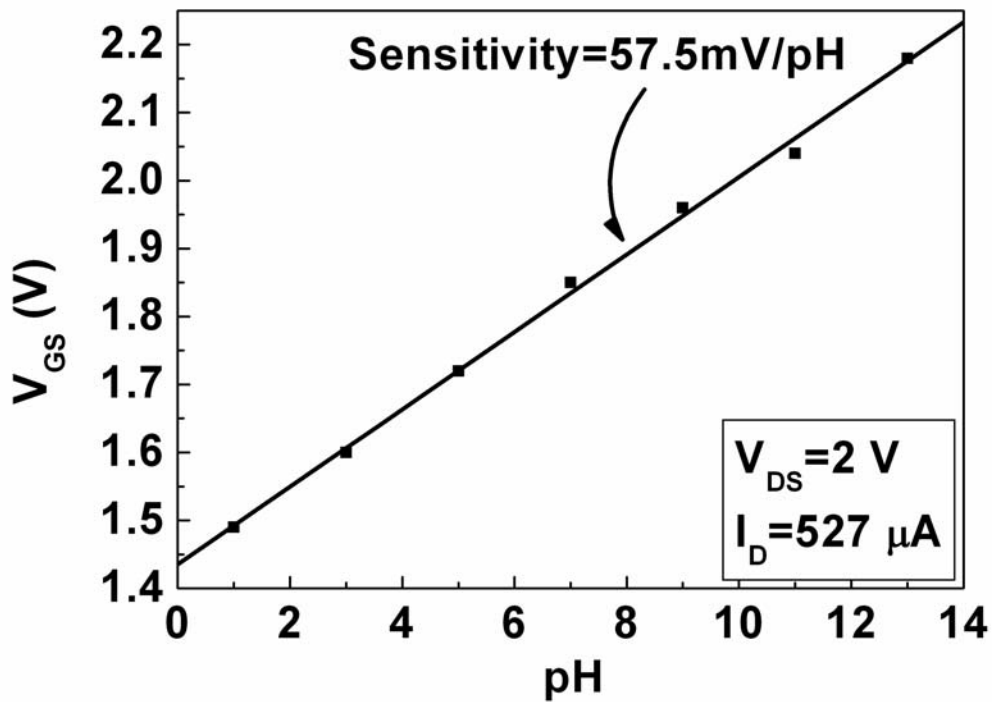


Figure 5-6 (b). Sensitivity of ZrO₂ gate ISFETs.

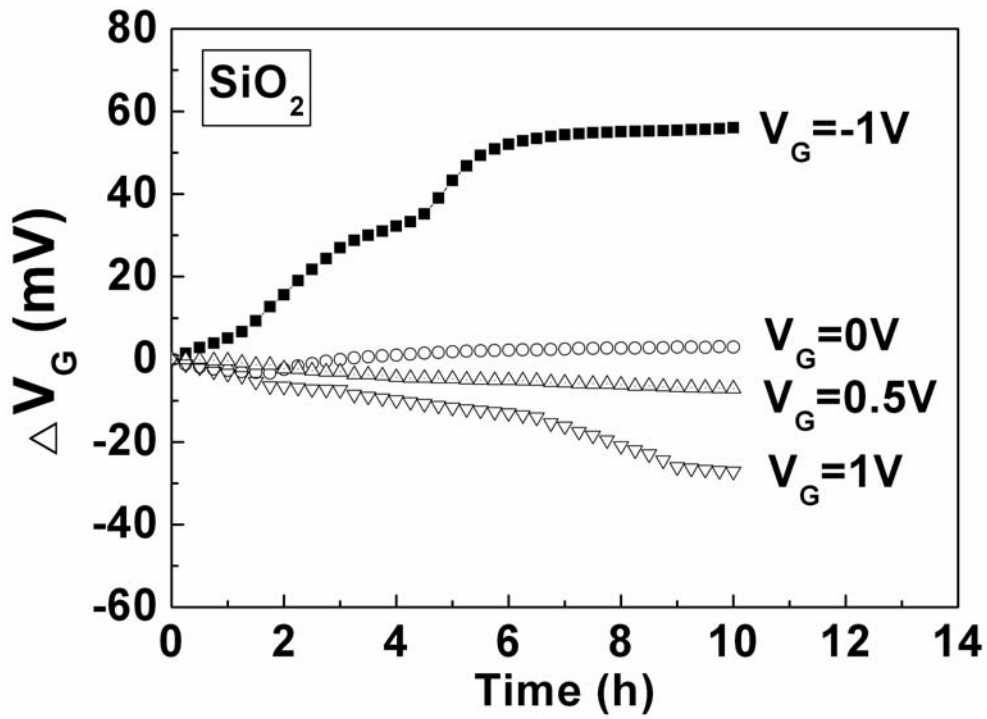


Figure 5-7 (a). Drift of SiO₂ gate ISFET with time.

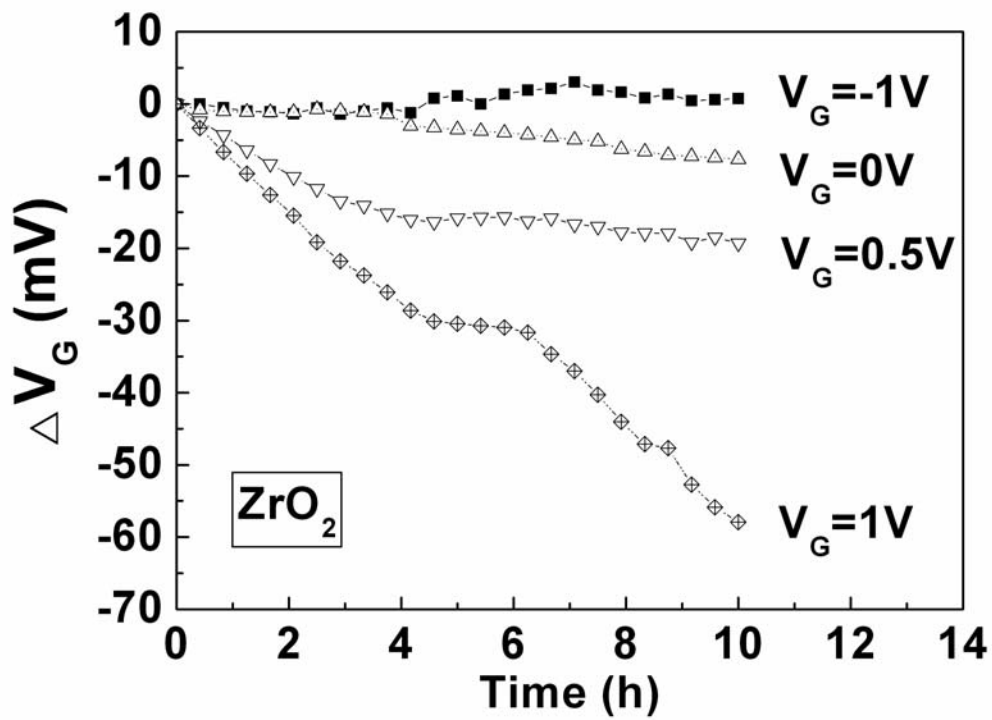


Figure 5-7 (b). Drift of ZrO₂ gate ISFET with time.

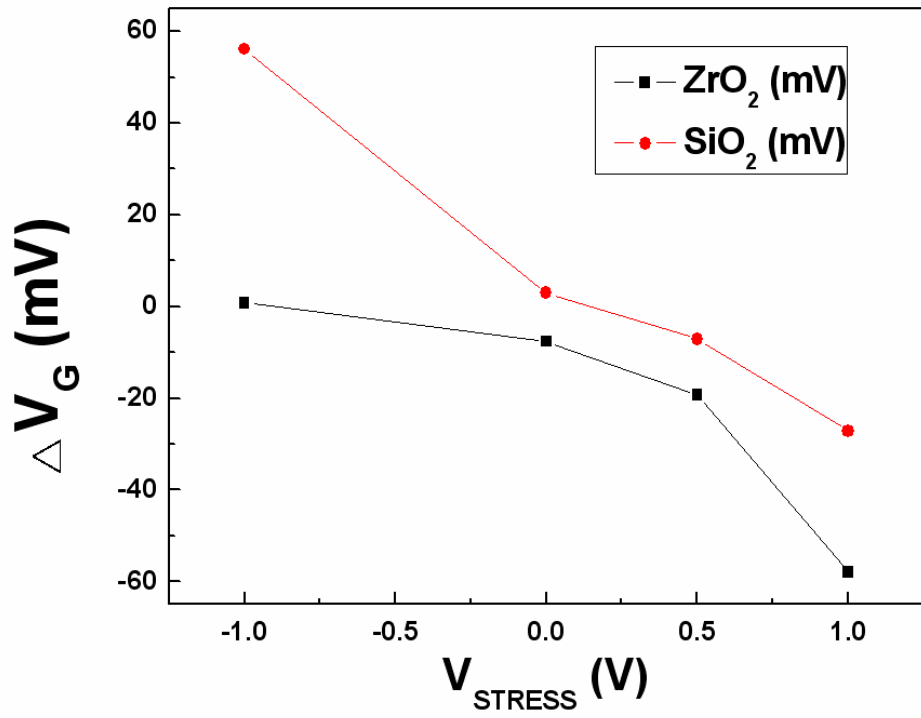


Figure 5-8 Relation of drift voltages and gate stress voltages.



Chapter 6

A Simple CMOS Compatible REFET for pH Detection by Post NH₃ Plasma Surface Treatment of ISFET

6.1 Backgrounds and Motivation

Ion-sensitive field effect transistor (ISFET) has been developed over 35 years, and the first sensitive membrane is silicon dioxide (SiO₂) that has first demonstrated by Bergveld in 1970 [1]. Since the SiO₂ gate ISFET appears instable sensitivity and large drift, a lot of sensitive layers, such as Al₂O₃, Ta₂O₅, SnO₂, TiN, a-WO₃, ITO and ZrO₂, are used as pH-sensitive membranes for the higher pH response and much stable drift voltage [2-9]. A conventional reference electrode (e. g. Ag/AgCl electrode) is always used in the measurement system. If we want to integrate the ISFET devices into a chemical micro system for in vivo analysis or become a part of lab-on-a-chip, the huge conventional reference electrode will be the biggest challenge. For this reason, there are several approaches that have been investigated to solve this problem.

One method to solve this problem is co-fabricated an Ag/AgCl electrode with ISFET, including a gel filled cavity and a porous silicon plug [10]. But this solution has a leaking path from reference electrode to solution that will reduce the device lifetime.

Another method is applying a differential measurement between an ISFET and an identical FET, which does not react on the ion concentration to be measured, called REFET. This method is deposition on top of the ISFET's surface one layer, which is an ion-unblocking membrane that is an insulating polymeric layer exhibiting independence on ionic strength. A commonly used material for ion-unblocking layer in REFET is polyvinylchloride (PVC) [11-12]. The REFET with PVC sensitive membrane has a smaller sensitivity of about 20mV/pH, but it will add some processes

to fabricate a REFET and is not compatible with integrated circuit (IC) technology.

The ZrO₂ prepared by dc sputtering process as a pH-sensitive membrane for ISFET is first developed in our laboratory [9]. In this work, we report a simple CMOS compatible REFET by post NH₃ plasma surface treatment on ZrO₂ gate ISFET. The electrical characteristics and pH response of the ZrO₂ gate ISFET is studied by the standard MOSFET measurement with HP 4156A. Without any unblocking layer to be deposited, the REFET also shows a very low sensitivity of about 28.3 mV/pH. With such ISFET/REFET differential pair, the conventional reference electrode can be replaced by a solid platinum electrode, which can fabricate in the same chip. By this way, a high integration of ISFET with IC fabricating can be realized in the future.

6.2 Experimental

6.2.1 Device Fabrication




Figure 6-1 shows the schematic diagram of the ZrO₂ gate ISFET, which is fabricated by the MOSFET technique. DC sputtering from a 4-inch diameter, and 99.99% purity of Zr in oxygen atmosphere deposited a 30nm thickness sensitive layer of ZrO₂ membrane onto the SiO₂ gate ISFET. The sputtering total pressure was 20 mTorr in the mixed gases Ar and O₂ for 200 minutes while the base pressure was 3× 10⁻⁶ Torr, and the rf power was 200W which the operating frequency was 13.56MHz. After a post NH₃ plasma treatment of ZrO₂ film, a REFET was completed with ISFET in a single chip. The detailed manufacturing processes were listed as follows:

- (1) RCA cleaning of 4-inch, p-type silicon wafer
- (2) Wet oxidation of silicon dioxide (600 nm, Figure 6-1(a))
- (3) Defining of S/D area with mask I and wet-etching of silicon dioxide by buffer oxide etcher (BOE)
- (4) Thermal growth of silicon dioxide as screen oxide (30 nm, Figure6-1 (b))

- (5) Phosphorus ion implantation and post annealing at 950°C (Figure 6-1 (c))
- (6) PECVD silicon dioxide for passivation layer (Figure 6-1 (d))
- (7) Defining of contact hole and gate region with mask II and wet-etching of silicon dioxide by BOE
- (8) Dry oxidation of gate oxide (10 nm)
- (9) DC sputtering 30nm thickness of ZrO₂ film and post annealing at 600°C (Figure 1 (e))
- (10) Defining of gate region with mask III and wet-etching of oxide by BOE
- (11) A post NH₃ plasma treatment by high-density plasma reactive ion etching (HDP-RIE) system
- (12) DC sputtering a 30nm thickness of ZrO₂ film with hard contact mask IV and post annealing at 600°C
- (13) Aluminum sputtering with hard contact mask V (600 nm, Figure 6-1 (f))

6.2.2 Packaging and Measurement

A container is bonded on the gate region of the ISFET/REFET by epoxy resin. Figure 6-2 shows the set up of measurement and the HP4156A Semiconductor Parameter Analyzer is used to measure the I_{DS} - V_{GS} characteristics of the ZrO₂ gate ISFET/REFET devices in the buffer solutions. All the measurement processes are carried out at the room temperature of 25 °C by a temperature control system, and placed in the dark box. Originally, a platinum film is prepared for the reference electrode, but in order to estimate the effect of reference electrode. A conventional Ag/AgCl reference electrode is used as a DC reference voltage to measure the ISFET and REFET systems. After the buffer solution is injected into the container, we will not measured until the ISFET/REFET is immersed in the buffer solution for 60 seconds to make sure that the devices are under steady situation.

6.3. Results and Discussion

6.3.1 The pH Sensitivity of the ZrO₂ Gate ISFET

The pH sensitivity of the ZrO₂ gate ISFET in pH = 1, 3, 5, 7, 9, 11 and 13 buffer solutions at room temperature is obtained by a HP4156A Semiconductor Parameter Analyzer. Figure 6-3 (a) shows that the I_{DS}-V_{GS} curves of ISFET are shifted in parallel with the pH concentration of the buffer solutions, and in the non-saturation region with V_{DS} = 2 V. The I_{DS}-V_{GS} curves represent the threshold voltage shift towards positive values with increasing pH values. After several times of measurements, a linear pH response of 56.7~58.3 mV/pH with the deviation of 3 % is obtained by calculating the shifts in the V_{GS} of the ISFET by a constant drain current at 527 μ A for different pH values. Figure 6-3 (b) shows the V_{GS} to pH values that can obtain a median pH response of 57.5 mV/pH by the slope of the linear fitted line. A 99.74 % of the root mean square can be obtained that represents the perfect response of the ZrO₂ gate ISFET.

6.3.2 The pH sensitivity of the ZrO₂ gate REFET

Figure 6-4 shows that the sensitivities of REFET are decreasing with increasing of NH₃ plasma treated times in 60 minutes. When the NH₃ plasma treated times reach 90 minutes, the sensitivity of REFET will increase slightly for the plasma bombardment. The individual sensitivities errors of ISFET and REFET are both about 1.5 mV in several times of measurements, and the tendency of the errors is the same in ISFET and REFET. Thus, the differential sensitivities of ISFET/REFET pairs are very stable with an error bar of about 0.2 mV. The differential sensitivities accuracy of the ISFET/REFET is about 0.7% (0.2/28). With the low sensitivities of REFET, we suggest the reason is that the surface sites [13] are passivated by H⁺ of plasma, resulting in the lower sensitivity of REFET. As a result, after the surface sites are decreasing with increasing plasma times, the sensitivities will be decreased.

Unfortunately if the times reach 90 minutes, the sensitivity will increase for the damage of surface by the plasma bombardment. Thus, the optimum time of NH_3 plasma process reaches 60 minutes in the experiment, the sensitivity of REFET will decrease to 27.6~29 mV/pH. And the differential sensitivity of the ISFET/REFET pair devices is 29.1~29.3 mV/pH.

6.4 Conclusion

A study of the ZrO_2 gate ISFET and REFET are first proposed as a pH-sensitive membrane pair. The sensing property of sensitivity is obtained by the $I_{\text{DS}}-V_{\text{GS}}$ measurement in a series of buffer solutions. The optimum time of NH_3 plasma process is 60 minutes for the REFET. The pH response is 56.7~58.3 mV/pH for ISFET and 27.6~29 mV/pH for REFET. The differential sensitivity about 29.1~29.3 mV/pH with an accuracy of 0.7% can be obtained for both the ISFET and REFET in the same drifting tendency. The ZrO_2 gate ISFET and REFET can be used in the pH range of 1 to 13 with perfect linear fitted line that is able to enable the ISFET devices more applications in many fields.

6.5 References

- [1] P. Bergveld, "Development of an ion sensitive solid-state device for neurophysiological measurements," IEEE Trans. Biomed. Eng. vol. 17, pp. 70–71, 1970.
- [2] S. D. Moss, C. C. Johnson, and J. Janata, "Hydrogen calcium and potassium ion sensitive FET transducers," A preliminary report, IEEE Trans. Biomed. Eng. vol. 25 pp. 49–54, 1978.
- [3] H. K. Liao, J. C. Chou, W. Y. Chung, T. P., and S. K. Hsiung, "Study on the interface trap density of the $\text{Si}_3\text{N}_4/\text{SiO}_2$ gate ISFET," Proceedings of the Third East Asian Conference on Chemical Sensors, Seoul, South Korea, pp. 394–400, November 1997.
- [4] L. T. Yin, J. C. Chou, W. Y. Chung, T. P., and S. K. Hsiung, "Study of indium tin oxide thin film for separative extended gate ISFET," Mater. Chem. Phys. vol.70 pp. 12-16, 2001.
- [5] P. Gimmel, B. Gompf, D. Schmeiosser, H. D. Weimhofer, W. Gopel, and M. Klein, " Ta_2O_5 gates of pH sensitive device comparative spectroscopic and electrical studies," Sensors and Actuators B vol. 17 pp. 195–202, 1989.
- [6] J. C. Chou and J. L. Chiang, "Study on the amorphous tungsten trioxide ion-sensitive field effect transistor," Sensors and Actuators B vol. 66 pp. 106-108, 1998.
- [7] T. matsuo and M. Esashi, "Methods of ISFET fabrication" Sens and Actuators vol. 1 pp. 77-96, 1981.
- [8] J. C. Chou and J. L. Chiang, "Ion sensitive field effect transistor with amorphous tungsten trioxide gate for pH sensing" Sens and Actuators B 62 pp. 81-87, 2000.
- [9] K. M. Chang, K. Y. Chao, T. W. Chou, and C. T. Chang, "Characteristics of Zirconium Oxide Gate Ion-sensitive Field-Effect Transistors" Jpn. J. Appl. Phys.

Vol. 46 No. 7A pp. 4334-4338 2007.

- [10] R. L. Smith and D. C. Scott, "An integrated sensor for electrochemical measurements," IEEE Trans. Biomed. Eng. BME vol. 33 pp. 83-90, 1986.
- [11] M. Chudy, W. Wroblewski, and Z. Brzozka, "Towards REFET," Sensors and Actuators B 57 pp. 47-50, 1999.
- [12] P. A. Hammond, D.R.S. Cumming, and D. Ali, "A single-Chip pH Sensor Fabricated by a Conventional CMOS Process," Proceeding of IEEE Sensors vol. 1 pp. 350-355, 2002.
- [13] D. E. Yates, S. Levine, and T. W. Healy, "Site-binding model of the electrical double layer at the oxide/water interface," J. Chem. Soc. Faraday Trans. I vol. 70 pp.1807-1844, 1974.



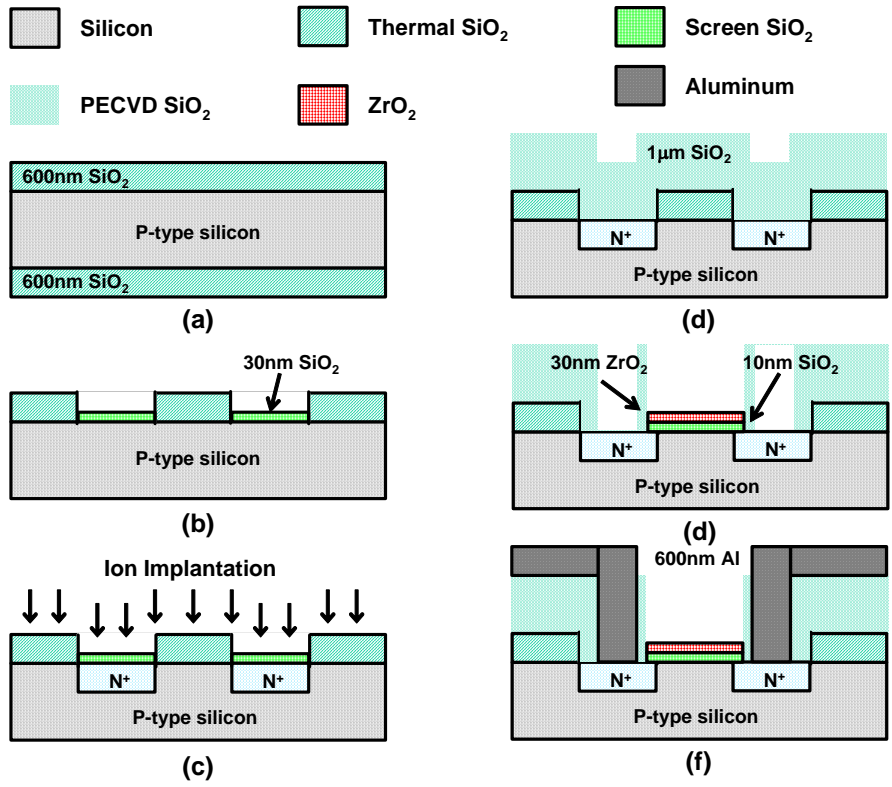


Figure 6-1 The schematic diagram of the ZrO₂ gate ISFET that is fabricated by the MOSFET technique.

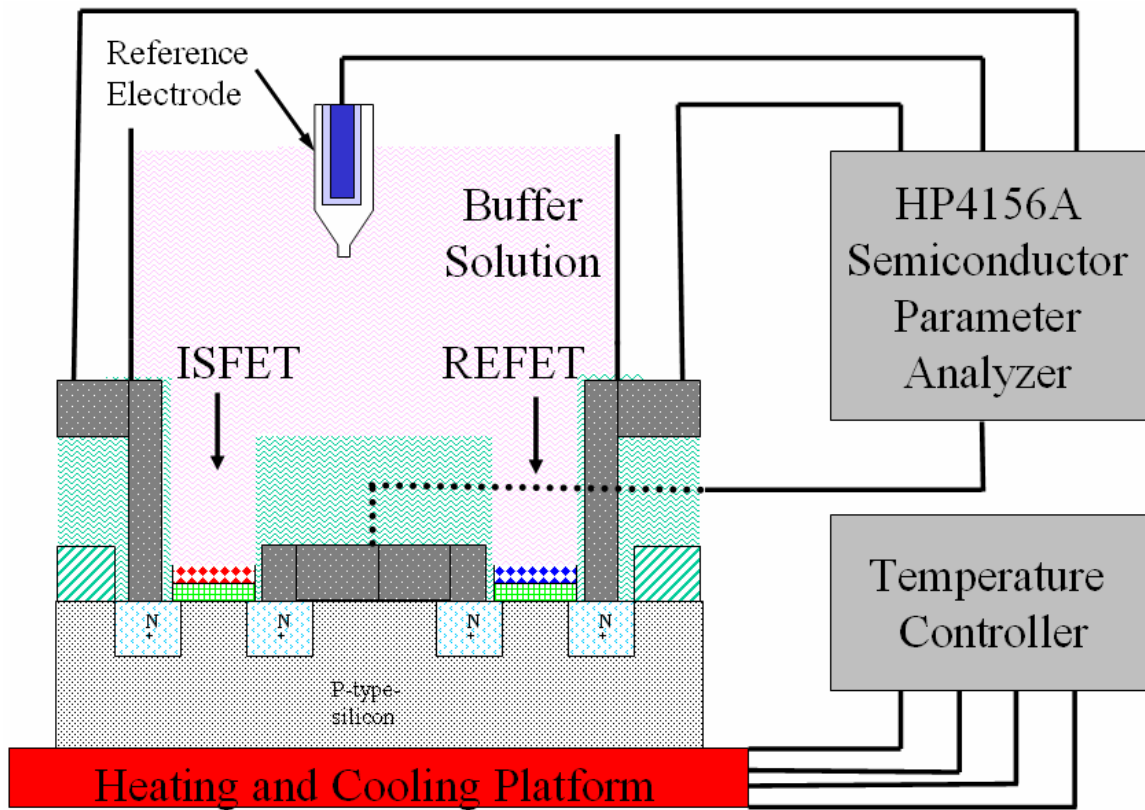


Figure 6-2 The set up of measurement with the HP 4156A Semiconductor Parameter Analyzer and Temperature controller.

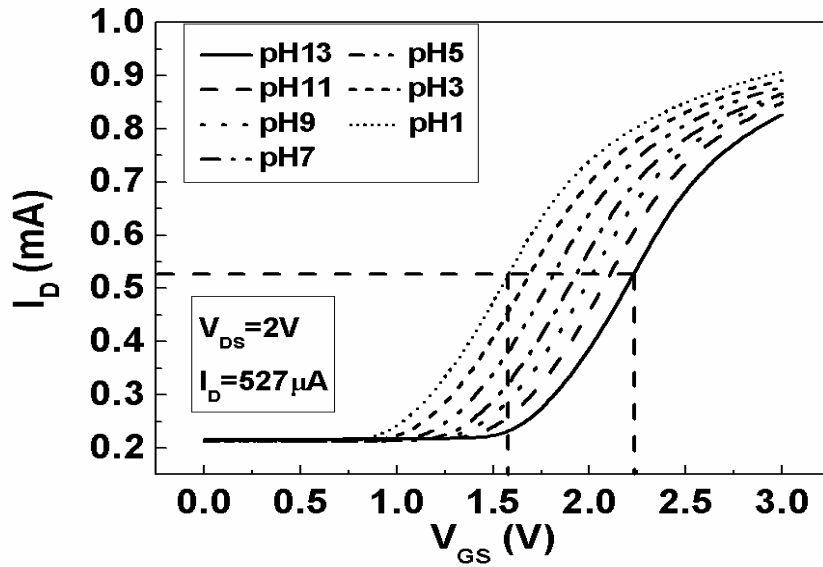


Figure 6-3 (a) The I_{DS} - V_{GS} curves that are shifted in parallel with the pH concentration of the buffer solutions, and in the non-saturation region with $V_{DS} = 2V$.

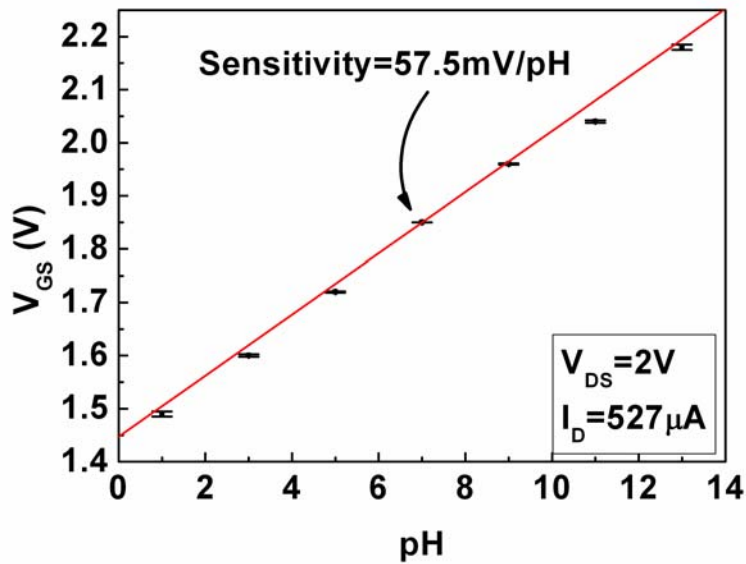


Figure 6-3 (b) The V_{GS} to pH values that can obtain a median pH response of 57.5 mV/pH by the slope of the linear fitted line.

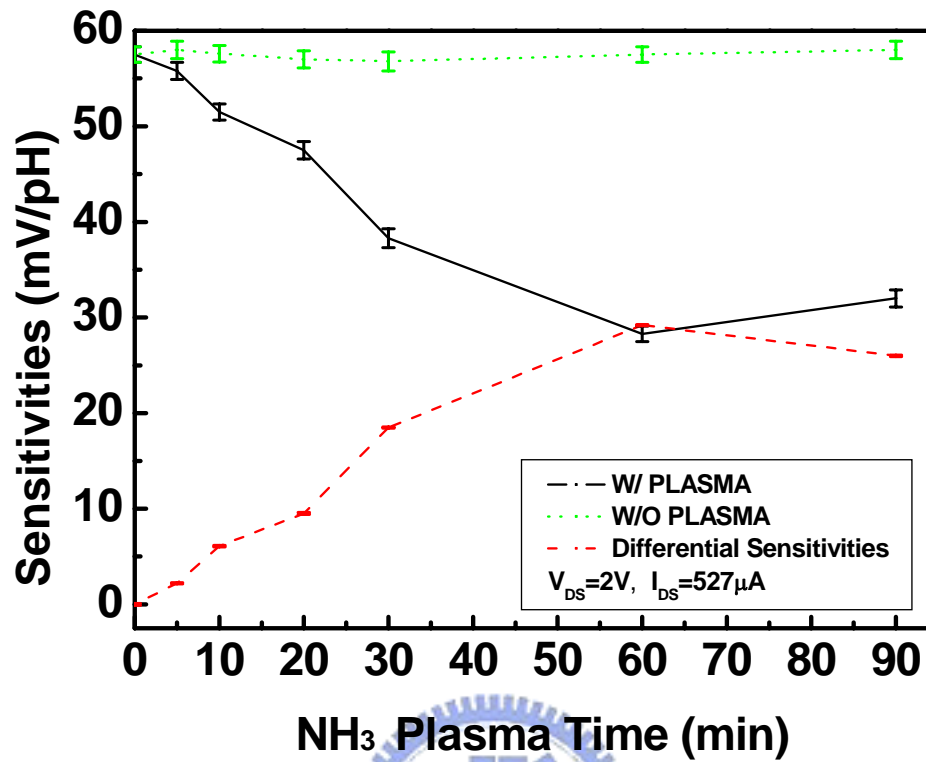


Figure 6-4 The sensitivities to post NH₃ plasma treatment time output characteristics of the ISFET(W/O Plasma), REFET(W/ Plasma) and ISFET/REFET pair (Differential Sensitivities) devices with $V_{DS}= 2V$ and drain current at $527 \mu A$.

Chapter 7

Conclusion and Future work

7.1 Conclusion

This study has investigated the ZrO_2 to be a membrane of ISFETs. And a REFET is used to control the effects of temperature and process deviation and proposed two methods to solve the unwanted effects.

The ZrO_2 membrane has been successfully applied as a pH-sensitive layer for ISFETs in Chapter 3. It exhibited an excellent response range of 56.7 mV/pH to 58.3 mV/pH. The ZrO_2 membrane prepared by DC sputtering was used as a pH-sensitive film that showed good surface adsorption with oxide and silicon. The pH sensitivities slightly decreased in 1 M NaCl solution; however, the device showed a perfect linear response of 52.5 mV/pH.

Furthermore, a REFET is used to control the effects of temperature and process deviation. After the calibration of REFET, a very stable sensitivity and intrinsic drift of SiO_2 gate ISFET can be obtained. It can be used to define the thickness of hydration layer that is introduced by the drift effect. Results of this study will show that the thickness of hydration is about 50 nm in SiO_2 membrane ISFET. It exhibits a stable response of 28~32 mV/pH. This method is a really simple way to find the thickness of hydration layer, and it will be useful in the study of the real mechanism in drift effect.

Finally, when the phenomenon of drift is understood, two methods are designed to reduce this effect. One is using the gate voltage to control drift voltage. It is a simple and cheap way to solve the drift problem is presented which describes the relation of drift and gate voltage. When various constant gate voltages are biased in

sensing layers with reference electrode. It obviously shows a strong relation of gate drifts and gate stress voltages. When the gate voltage is controlled as 0.5 V, the drift voltage of SiO₂ gate ISFET will decrease from 56.12 to 2.94 mV in ten hours measurement. The improvement of drift voltage reaches 94.8%. When the gate voltage is controlled as -1 V, the drift voltage of ZrO₂ gate ISFET will also decrease from -57.94 to 0.76 mV. The improvement of drift voltage reaches 98.7%.

Another method is using a REFET to reduce the drift effect. A simple CMOS compatible REFET for pH detection by post NH₃ plasma surface treatment of a ZrO₂ membrane ISFET has been developed. It is a novel study that has latent capacity to integrate the ISFET devices into a chemical micro system for in vivo analysis or become a part of lab-on-a-chip. With the fixed current measurement by HP4156, we can get not only the individual sensitivities of ISFET and REFET, but also the differential sensitivities of ISFET/REFET pair. The ZrO₂ membrane ISFET exhibits an excellent response of 56.7~58.3mV/pH with deviation of 3% and the REFET shows a small response of 27.6~29 mV/pH with a deviation of 5%. Using this ISFET/REFET differential pair, we can get a very stable differential sensitivities of 29.1~29.3 mV/pH with a small deviation of 0.7%. This result indicates that the research not only makes the ISFET integrate into a micro system in a simple way possible, but also increases the stability of sensitivity.

7.2 Future Work

Even though the drift voltage could be measured easily here, we did not collect enough data to develop a new model to predict how deep of the hydration layer would be. The mechanism of drift should be modeled and understood clearly. And we proposed two methods to solve the drift effect to make the system become more stable and small. But we did not realize the system on one chip. We need to measure the out

put voltage by a HP4156A. It is not a good system to be used for everyone. Thus, the next step of our lab is going to develop a smart chip that integrates all the components in only one chip. That is the finally target of this study. When the single chip is realized, we will change the sensing membranes to be a ChemFET that will have more applications in biology. Hence, the device will become a useful one in the future.

